Lower Aeronian triangulate monograptids of the genus *Demirastrites* Eisel, 1912: biostratigraphy, palaeobiogeography, anagenetic changes and speciation

Petr Štorch & Michael J. Melchin

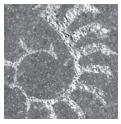

Bed-by-bed sampling of the lower Aeronian black shale succession exposed at the Hlásná Třebaň section in the Prague Synform of the Czech Republic has provided a rich and continuous fossil record of biostratigraphically important "triangulate monograptid" graptolites referred to the genus *Demirastrites* Eisel, whose diagnosis is revised. Eight morphological forms assigned to four species, including the biozonal index taxa *Demirastrites triangulatus* (Harkness) and *D. pectinatus* (Richter), as well as *D. major* (Elles & Wood) and *D. campograptoides* sp. nov., are distinguished and described. Also documented are patterns of morphological change within species that we interpret to be anagenetic changes, as well as apparent patterns of morphological divergence that we interpret to represent speciation events. The proposed phylogeny suggests that the *D. triangulatus* lineage underwent significant anagenetic changes throughout its range before it split at the base of the *pectinatus* Biozone and gave rise to *D. pectinatus*, which then underwent further anagenetic changes between its early and late forms. At a slightly later stage, in the lower *pectinatus* Biozone, the *D. triangulatus* stem lineage underwent further significant changes, giving rise to *D. major*, which then saw further significant anagenetic changes before it became extinct in the middle *pectinatus* Biozone, well below the highest occurrence of *D. pectinatus*. *D. campograptoides* is a rare and apparently short-ranging species, thus far recorded only from Bohemia, derived from either early *D. triangulatus* or its direct ancestor. Reconsideration of the species' records worldwide suggest that none of these lower Aeronian forms was truly cosmopolitan. • Key words: graptolite, Silurian, Aeronian, zonal index species, stratigraphy, taxonomy, evolution, intraspecific variability, Prague Synform, Czech Republic.

Štorch, P. & Melchin, M.J. 2018. Lower Aeronian triangulate monograptids of the genus *Demirastrites* Eisel, 1912: biostratigraphy, palaeobiogeography, anagenetic changes and speciation. *Bulletin of Geosciences 93(4)*, 513–537 (12 figures, 1 table). Czech Geological Survey, Prague. ISSN 1214-1119. Manuscript received October 31, 2018; accepted in revised form December 3, 2018; published online December 20, 2018; issued December 20, 2018.

Petr Štorch, Institute of Geology CAS, Rozvojová 269, Praha 6, 16502, Czech Republic; storch@gli.cas.cz • Michael J. Melchin, Department of Earth Sciences, St. Francis Xavier Univeristy, Antigonish, Nova Scotia, B2G 2W5, Canada

Global correlation of Silurian rocks relies, to a large extent, on planktonic graptolites, the most common and diversified macrofossils to be found in anoxic black shales, which are widespread in off-shore depositional settings, particularly in the lower part of the Silurian System. High-resolution correlation, particularly quantitative stratigraphical correlation based upon semi-automated (Shaw's graphic correlation: Shaw 1964, Cooper & Lindholm 1990, Fan *et al.* 2013) and automated systems (CONOP: Sadler *et al*. 2003, 2011; Sadler 2004; Cooper *et al*. 2014 and Horizon Annealing: Sheets *et al*. 2012, Melchin *et al*. 2016a) have demanding requirements for primary data input. Densely sampled sections with abundant and highly diversified graptolite faunas are just one step on the way to maximum resolution in stratigraphy and correlation, which also relies critically on the correct taxonomic assignment of the taxa involved. Modern taxonomic revisions are needed not only for the purpose of high-resolution stratigraphy and correlation, but also correct determination of the taxa is a primary prerequisite for any palaeobiogeographical analysis, particularly when closely similar taxa occur in a similar, but not always the same, stratigraphical interval in different palaeobiogeographical provinces.

The present study focusses on the systematic revision of lower Aeronian monograptids with proximal rastritiform to sub-rastritiform thecae and non-overlapping, sub-rastritiform to high-triangular distal thecae with hooked apertures that are transversely extended into a pair of lateral apertural processes. These graptolites are of particular importance in lower Aeronian graptolite biostratigraphy

worldwide. They were often reported by earlier authors as an informal group of "triangulate monograptids" and assigned to the broadly based genus *Monograptus* (see *e.g.* Sudbury 1958, Rickards 1970, Hutt 1975, Rickards *et al.* 1977). New insights into graptolite thecal morphologies and recognition of several similar monograptid genera – *Campograptus* (Obut *et al.* 1968), *Lituigraptus* (Ni, 1978) and *Torquigraptus* (Loydell, 1993) – restricted some of the remaining "triangulate monograptids" to species with rhabdosomal and thecal forms that correspond with those of the genus *Demirastrites* (Eisel, 1912), as diagnosed by Přibyl & Münch (1942) and Štorch (2015).

The first appearance datum of *Demirastrites triangulatus* (Harkness, 1851), the type species of the genus and biozonal index fossil of the lowermost Aeronian graptolite biozone, has been widely used as a marker of the base of the Aeronian Stage (*e.g.* Štorch 1994, Melchin *et al.* 2012, Štorch *et al.* 2018). Although some fragmentary specimens with similar isolated thecae, assigned questionably to *Demirastrites brevis* (Sudbury, 1958), have been found in strata as low as the topmost Rhuddanian of the Rheidol Gorge section (uppermost *Coronograptus cyphus* Biozone – Melchin *et al.* 2018), the first appearance and abrupt proliferation of *D. triangulatus* marks lowermost Aeronian strata and began a rapid Aeronian expansion of monograptids with more-or-less isolated and hooked metathecae (*Demirastrites*, *Campograptus*, *Rastrites*, *Lituigraptus*, *Torquigraptus* and some species provisionally retained in "*Monograptus*"). Although *Demirastrites triangulatus* and its eponymous biozone have been reported from Siberia (*e.g.* Obut *et al.* 1968) and China (Chen & Lin 1978, Anhui Geological Survey 1982, Li 1995), specimens assigned to *D. triangulatus* in Siberia and China differ from the European form in their lesser dorso-ventral width (DVW), less prominent thecal apertural processes and some other morphological details. *Demirastrites pectinatus* (Richter, 1853), likely a descendant of *D. triangulatus*, has been employed as an index species of a graptolite biozone overlying the *D. triangulatus* Biozone in peri-Gondwanan Europe (*e.g.* Bouček 1953, Štorch 1994, Loydell 2012) and as a subzonal index in Arctic Canada (Melchin 1989, Melchin & Holmden 2006). It is the senior synonym of *Monograptus fimbriatus* (Nicholson, 1868) (*e.g.* Bjerreskov 1975), commonly reported from the same stratigraphical interval in Britain, which was assigned to the upper *D. triangulatus* Biozone by Zalasiewicz *et al.* (2009).

A continuous, stratigraphically ordered morphological series of "triangulate monograptids" assigned to *Monograptus fimbriatus*, *M. raitzhainensis* and *M. triangulatus* was first recorded and interpreted by Challinor (1945) from Rheidol Gorge, Wales. Based on more detailed systematic study of larger, more densely sampled collections of well-preserved, pyrite-infilled specimens from the Rheidol Gorge section, Sudbury (1958) revised

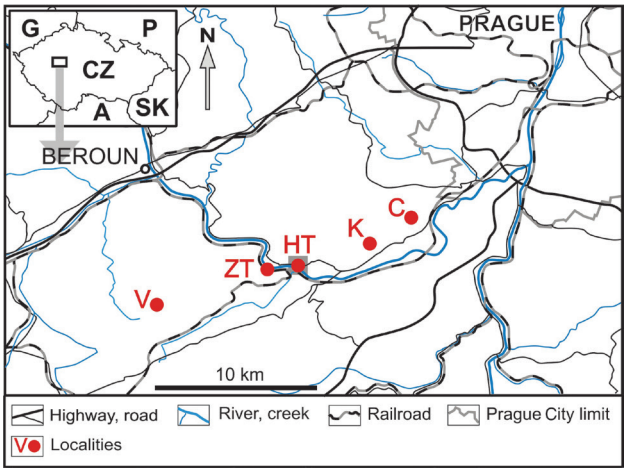

Figure 1. Location map of the Hlásná Třebaň section and other localities within the Prague Synform. Abbreviations: HT – Hlásná Třebaň (49° 55′ 22.9″ N, 14° 12′ 43.0″ E); ZT – Zadní Třebaň (49° 55′ 10.5″ N, 14° 11′ 5.8″ E); K – Karlík (49° 56′ 30.0″ N, 14° 16′ 8.6″ E); C – Černošice (49° 57′ 27.1″ N, 14° 18′ 23.0″ E); V – Všeradice (49° 52′ 36.3″ N, 14° 6′ 12.9″ E). See Štorch (2015) and Štorch *et al.* (2018) for locality details.

the interpretions of the proposed lineages among the taxa preserved at that section and brought substantial progress in our understanding of the morphological details and the stratigraphical succession of the "triangulate monograptids". In particular, Sudbury (1958, fig. 24) proposed a hypothesis for the evolution of members of the *D. triangulatus* group based on data from the Rheidol Gorge section. It is important to note that Sudbury (1958) had named the various members of the *triangulatus* group as subspecies of *Monograptus separatus*, but later corrected this, recognizing that the name *Monograptus triangulatus* had priority over *M. separatus* (Sudbury 1959). Her study of the evolutionary relationships among the members of the *Monograptus triangulatus* group spanned the lower part of the *gregarius* Biozone, an interval that is now recognized as the lower to upper part of the *M. triangulatus* Biozone of Zalasiewicz *et al.* (2009), which correlates with the *D. triangulatus* Biozone and lower part of *Demirastrites pectinatus* Biozone of continental Europe (see Melchin *et al.* 2018). Lower Aeronian graptolites of the Rheidol Gorge section, a locality proposed as one of the candidate sections for the new base Aeronian GSSP (Melchin *et al.* 2016b, 2018), are confined to a number of black-shale bands interbedded with graptolite-barren mudstones (Jones 1909, Sudbury 1958, Cullum & Loydell 2011, Melchin *et al.* 2018). As a result of the unfossiliferous intervals, the record of graptolite evolution is not complete in that section. Rhabdosomes collected from some fossiliferous bands are preserved in full relief but affected by varying degrees of brittle cleavage deformation. Also, some apertural details are not completely preserved in the pyrite internal moulds. No chemically etched specimens of undoubted members

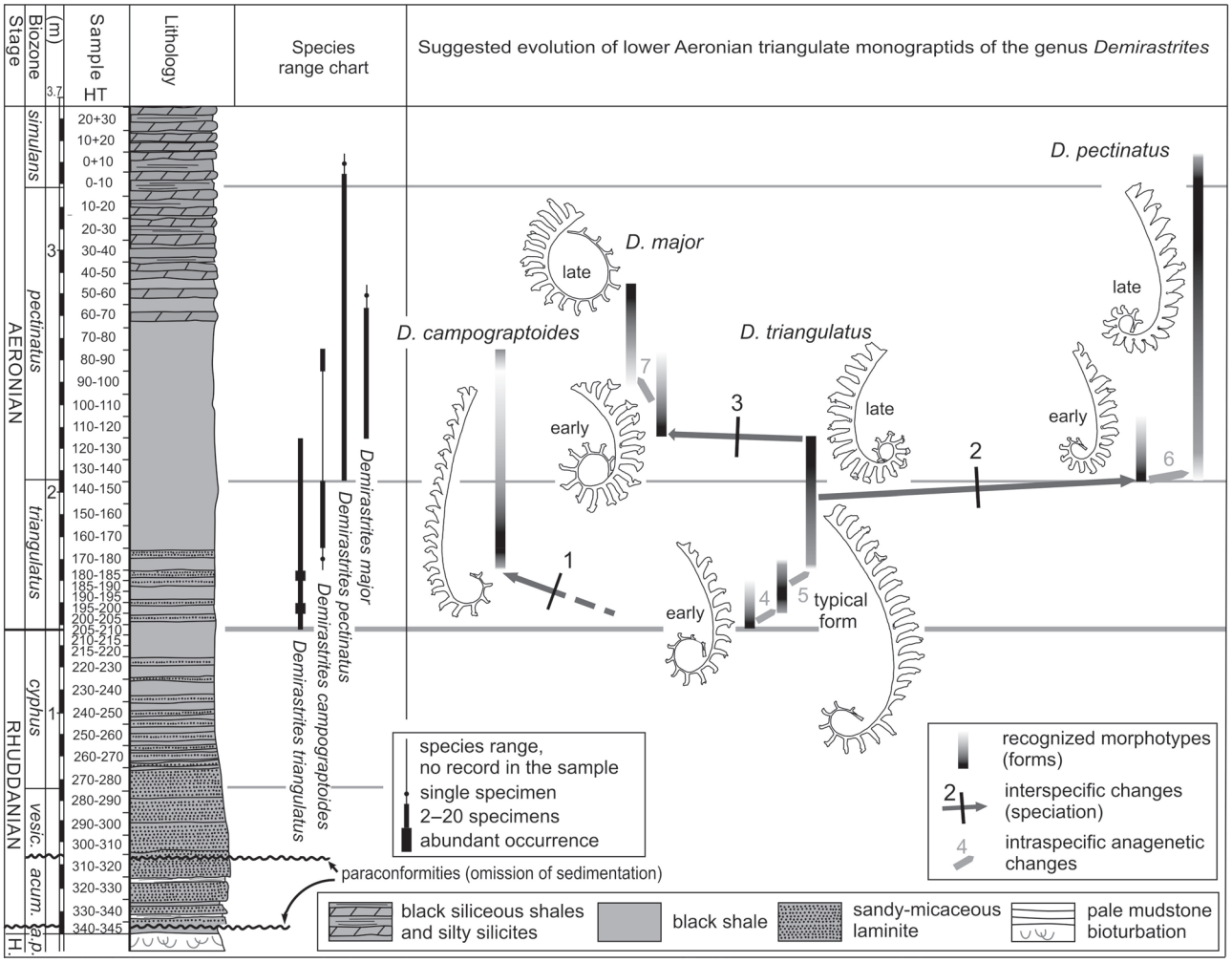

Figure 2. Stratigraphical ranges and proposed evolution of lower Aeronian demirastritids based on the fossil record from the Hlásná Třebaň section. Morphological modifications attributed to speciation: 1 – early derivation of *D. campograptoides* from demirastritid stem-line through rapid transition from a few rastritid proximal thecae to robust, slightly hooked distal thecae is tentatively suggested; 2 – origin of *D. pectinatus* from late form of *D. triangulatus* marked by prothecal shortening and rapid decrease of thecal isolation, increasing thecal width (robustness), significant shortening of lateral apertural processes and lessening of the DVW and of proximal dorsal curvature of the rhabdosome; 3 – origin of *D. major* resulted in more densely spaced, ventrally curved sub-rastritiform metathecae, which became significantly longer at the expense of the prothecal part (greater DVW and lesser 2TRD in mesial and distal part of the rhabdosome), and maximum extension of lateral apertural processes. Gradual shift in some of the morphological characters has been ascribed to anagenetic changes; 4 – typical form of *D. triangulatus* developed from the early morphotype by developing several fully rastritiform thecae near the proximal end, and more densely spaced thecae in the distal part of the rhabdosome. Theca 1 and th2 became higher, the rhabdosome width increased more rapidly; 5 – relatively short ranging typical form was soon replaced by specimens of the late form with tightly coiled proximal part and more densely spaced and less inclined thecae furnished with more strongly developed apertural processes; 6 – *D. pectinatus* recorded progressive lessening of mesial and distal DVW in stratigraphically higher specimens, in part due to lower thecal inclination, and further lessening of thecal isolation; 7 – *D. major* went through progressive straightening and remarkable protraction of the proximal part having proximal prothecae substantially elongated at the expense of metathecae. Abbreviations: *p*. – *persculptus* Biozone; *a*. – *ascensus* Biozone; *acum*. – *acuminatus* Biozone; *vesic*. – *vesiculosus* Biozone; H – Hirnantian. Section log and sampling after Štorch *et al*. (2018). Simplified drawings of recognized morphotypes (×2) are based upon real specimens.

of the *D. triangulatus* group have been previously reported either from Wales or elsewhere.

Detailed examination of the present material from the Hlásná Třebaň section, supplemented with further collections from Všeradice, Černošice and Karlík (Fig. 1), as well as some specimens from Spanish and Austrian localities, has shed more light on high-resolution biostratigraphy, correlation, palaeobiogeography, as well as proposed anagenetic changes and speciation events in the lower Aeronian monograptids assigned to the genus *Demirastrites* Eisel, 1912. *Demirastrites extremus* and *D. predecipiens*, both described by Sudbury (1958, as subspecies of *Monograptus separatus*), and ?*Demirastrites similis* (Elles & Wood, 1913) have not been recognized

in our collections, nor have they been recorded with certainty elsewhere in continental Europe. *Demirastrites triangulatus separatus* (Sudbury, 1958) is not regarded here as a distinct subspecies of *D. triangulatus* (see discussion of this species below).

The present study, based on bed-by-bed sampling of the continuously fossiliferous Hlásná Třebaň section, with abundant, albeit flattened specimens of *Demirastrites*, has enabled detailed insights into the morphological changes through the stratigraphical ranges of the species present: *D. triangulatus* (Harkness), *D. major* (Elles & Wood), *D. pectinatus* (Richter) and *D. campograptoides* sp. nov. (Fig. 2). Specimens assigned to "*Demirastrites*" *brevis* (Sudbury 1958) (originally named *Monograptus toernquisti brevis*) also occur in the *D. triangulatus* Biozone at Hlásná Třebaň (Štorch *et al*. 2018). This taxon is not included in this study because our available specimens are too sparse and incomplete, consisting only of near-proximal to mesial fragments, for complete documentation of its morphology and phylogenetic relationships. In addition, although the distal thecae of this species, as it is known from the type material, are sub-rastritiform, similar to those of early forms of *D. triangulatus* (although shorter), the proximal three to four thecae are highly axially elongate, so there is some question as to whether this species should be assigned to *Demirastrites*.

Material and methods

This study is based mainly on 218 specimens of *Demirastrites*, which were well enough preserved for detailed morphometric analysis, collected from the *Demirastrites triangulatus* and *D. pectinatus* biozones, sampled bed-by-bed from the base Aeronian GSSP candidate section at Hlásná Třebaň (Štorch *et al*. 2018). This material has been complemented by other less complete and/or less well-preserved specimens from Hlásná Třebaň, as well as specimens from several other localities within the Prague Synform (Barrandian area of central Bohemia, Czech Republic): Všeradice (Štorch 2015), Zadní Třebaň and Černošice (Štorch 1994). Further specimens employed in this study came from measured lower Aeronian sections in southwestern Spain (El Pintado section, see Loydell *et al*. 2015) and the Carnic Alps (Oberbuchach Nölblinggraben section, Jaeger & Schönlaub 1977). The studied specimens are compared with published, well-documented collections from Thuringia (Schauer 1971), Brittany (Piçarra *et al*. 2009), southwestern Sweden (Törnquist 1899), Bornholm (Bjerreskov 1975, Loydell *et al*. 2017), Latvia (Loydell *et al*. 2003), Lithuania (Paškevičius 1979) and the UK (Elles & Wood 1913, Sudbury 1958, Rickards 1970, Hutt 1975 and MJM personal observation).

In order to complete the systematic revision, vital for correlation and subsequent palaeobiogeographical studies, we also examined specimens from Morocco (PS personal observation, see also Willefert 1963), sections in South China, including material deposited in Nanjing Institute of Geology and Palaeontology, collections from northwestern and Arctic Canada (see also Lenz 1982, Melchin 1989), and published data from Siberia (Obut *et al*. 1965, 1967, 1968).

Graptolites from Hlásná Třebaň and other Czech sections are preserved as flattened impressions, either carbonized or partly pyritized. Spanish specimens are also flattened but the rhabdosomal material is overgrown by a pale ?chloritic mineral.

For a better understanding of the thecal morphology, study of the flattened material has been supplemented by observations on fragments of *Demirastrites* ex gr. *triangulatus* chemically isolated from limestone nodules, studied by scanning electron microscopy, from the *pectinatus–triangulatus* Subzone of the Cape Manning section, Cornwallis Island, Arctic Canada (see Melchin *et al*. 2017, for locality details).

The detailed morphological and morphometric analysis, based upon 43 characters, was performed using the 218 most complete and/or best preserved rhabdosomes from Hlásná Třebaň. Additionally, 38 specimens from Všeradice, Zadní Třebaň and Černošice sections and 10 specimens from the Spanish El Pintado Section, were used in determining the ranges of variation in thecal form and dimensions for the species descriptions. In the species decriptions (M) indicates mean value and (n) indicates number of specimens used for calculation of mean values of the respective characters. Mean values were calculated only in those cases where ten or more measurements were available for a particular character. Specimens were photographed with an Olympus BX16 microscope fitted with a Canon EOS 1200D camera, line drawings were made using a camera lucida and traced using Adobe Photoshop software.

The following characters have been measured and/or described (see Fig. 3 for graphic explanation): width of the sicular aperture; sicula length; distance between the sicular aperture and point of origin of th1; location of the sicular apex relative to the base of the dorsal wall of the first metatheca; dorso-ventral width of the rhabdosome (DVW) at th1, 2, 3, 4, 5, 10, and distally; two thecae repeat distance (2TRD *sensu* Howe 1983) at th2, 3, 5, 10, and distally; total axial length of th1; prothecal tube length of th1, 3, 5 and 10; prothecal width at base of th2, 5, 10 and in distal thecae; metathecal width at the midpoint of the metathecal height at th2, 5, 10 and in distal theca; curvature of the ventral prothecal wall at th 2, 5 and 10; tapering of the metathecal tube at th2, 5, 10 and in distal thecae; ventral curvature of metathecae; maximum length of the lateral apertural processes in the proximal thecae (th1–5) and distal thecae; angle of metathecal inclination at th2, 5, 10 and in distal thecae; angle of rhabdosome curvature

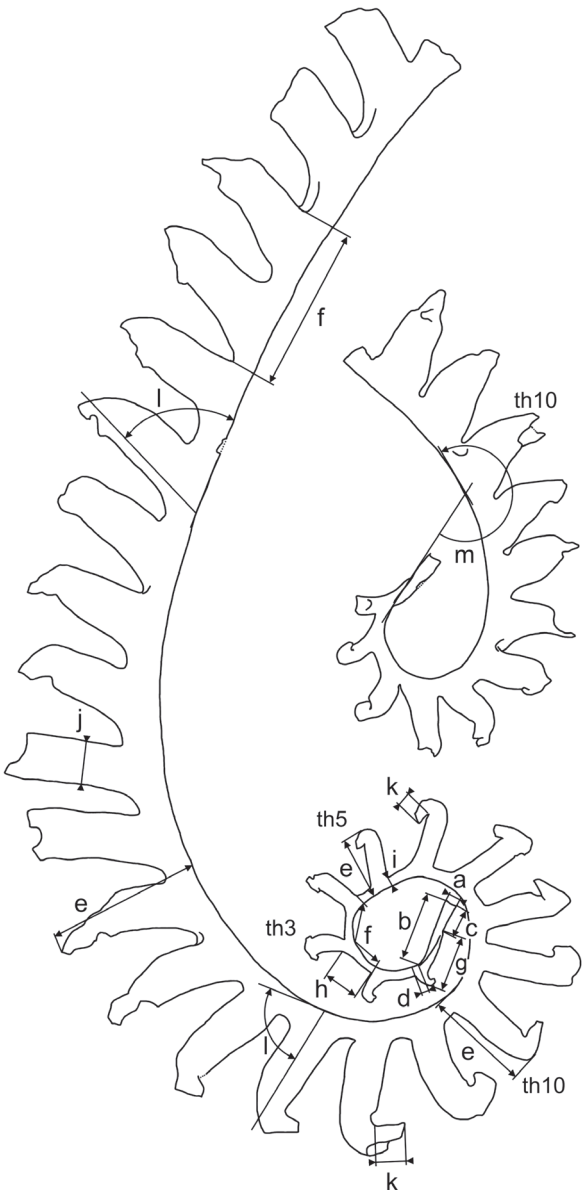

Figure 3. Some of the characters measured on rhabdosomes in this study: a – width of the sicular aperture; b – sicula length; c – distance between the sicular aperture and point of origin of th1; d – location of the sicular apex related to dorsal wall of the first metatheca; e – dorso-ventral width of the rhabdosome (DVW) at th1, 2, 3, 4, 5, 10, and distally; f – two thecae repeat distance (2TRD) at th 2, 3, 5, 10, and distally; g – total axial length of th1; h – length of ventral prothecal wall at th1, 3, 5 and 10; i – prothecal width at base of th2, 5, 10 and in distal thecae; j – metathecal width at midpoint of the metathecal height at th2, 5, 10 and at distal theca; k – length of lateral apertural processes in proximal thecae (th1–5) and distal thecae; l – angle of metathecal inclination at th2, 5, 10 and at distal thecae; m – angle of rhabdosome curvature between th 1 and th10.

between the sicula and th10; and, ordinal number of the most distal rastritiform or sub-rastritiform theca.

The graptolite material for this study from the Prague Synform is housed in the Czech Geological Survey, Prague in a collection prefixed PŠ, and Spanish specimens prefixed MGM are housed in Museo Geominero, Instituto Geológico y Minero de España, Madrid. Type specimens prefixed GSM are housed in British Geological Survey, Keyworth; specimen prefixed SM is housed in Sedgwick Museum, Cambridge; a type specimen prefixed BGR X is housed in the Bundesanstalt für Geowisseschaften und Rohstoffe, Berlin. Specimens from Arctic Canada prefixed ROM are housed in the Royal Ontario Museum, Toronto, and those prefixed GSA are in the type collections of the Geological Survey of Canada in Ottawa.

Comments on overall morphology and taphonomy

All species of *Demirastrites* show at least some gradient in their thecal form from the proximal to distal end. The terminology that we employ in this study pertaining to overall thecal form, as well as apertural form, is illustrated in Fig. 4. We restrict the term "rastritiform" thecae to those that possess parallel-sided prothecae and straight, parallel-sided metathecae that emerge at a high angle from the prothecae. If there is a parallel-sided to gradually widening protheca whose ventral wall is clearly distinct (marked by a point of inflection – we refer to this portion of the prothecae as "prothecal tubes") from that of the more erect metatheca but the metathecae are tapering and/or curved, then these are referred to as "sub-rastritiform" thecae. If the ventral wall of the protheca is highly inclined and/or strongly concave and merges smoothly into that of the metatheca with no distinct prothecal tube, and the thecae are high (significantly higher than wide) and triangular in overall form, then the thecae are referred to as "high-triangulate".

The thecal morphology most commonly associated with the genus *Demirastrites* is fully rastritiform thecae proximally, gradually changing to high-triangulate distally. Many specimens of *D. triangulatus* and *D. major* display this typical morphology. However, some specimens that we have assigned to *D. triangulatus* show slightly tapering and/or slightly curved (sub-rastritiform) (Fig. 4A) proximal metathecae. Many specimens of *D. major* also show slightly curved proximal metathecae. *Demirastrites pectinatus* and *D. campograptoides* are both characterized by possessing sub-rastritiform thecae proximally. In the case of the former species, there are only a few sub-rastritiform thecae before they change to a high-triangulate form (Fig. 4A). There are also specimens of *D. triangulatus* and *D. major* that appear to retain the sub-rastritiform thecae, with distinct prothecal tubes, into the distal part of the rhabdosome. It is difficult to know how much of this apparent variation in form of the prothecae is the result of slight differences in the mode of flattening compression, but similar intraspecific variations in prothecal form can

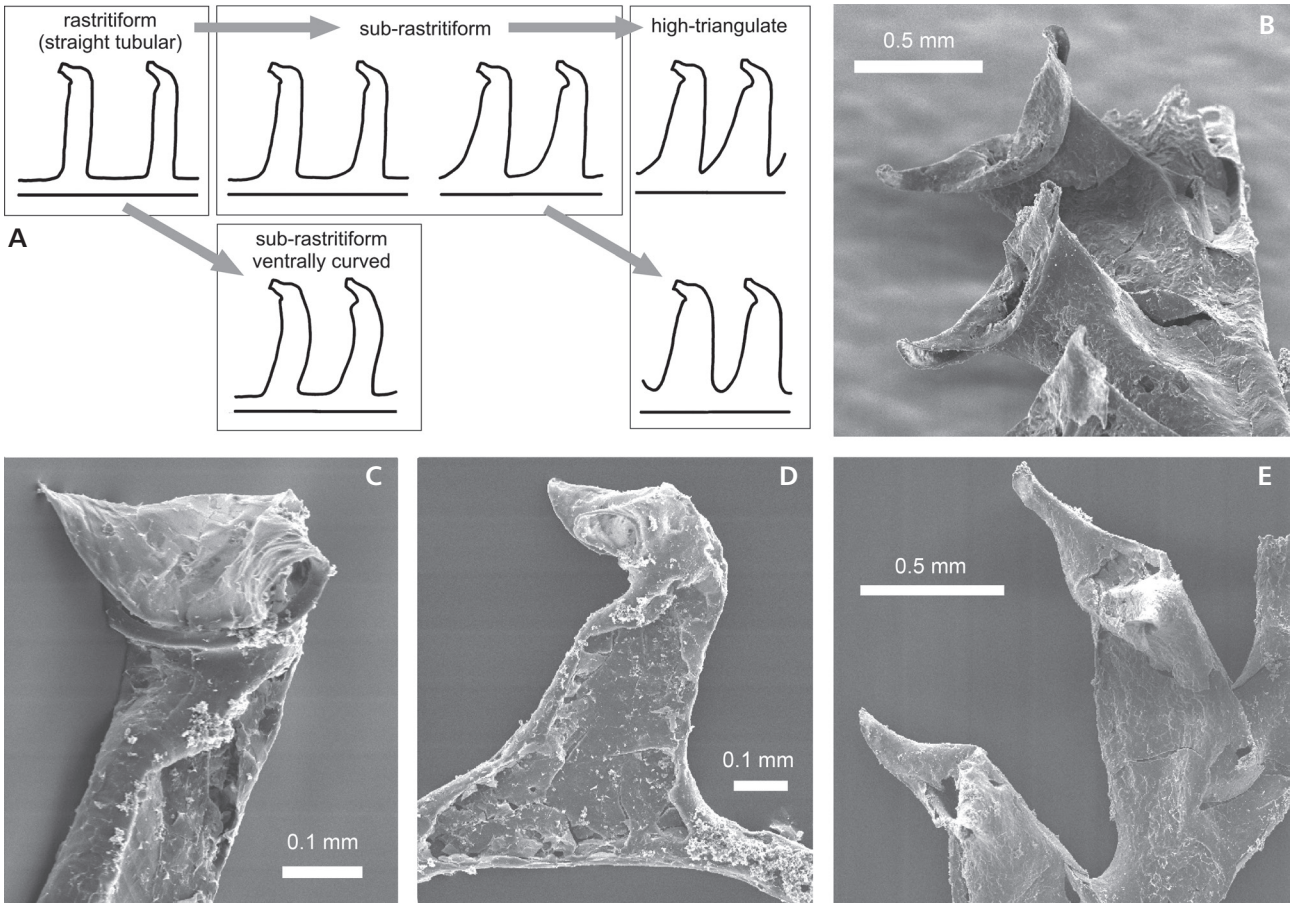

Figure 4. Thecal morphology of the lower Aeronian demirastritids. • A – terminology of thecal profile applied in this study. • B–E – thecal form and apertural details preserved in fragmentary *Demirastrites* ex gr. *triangulatus* chemically etched by Dawson (2007) from limestone nodule of the Cape Manning section, Cornwallis Island (sample MCM2 – 98, 47.9–48.0 m; see Melchin *et al.* 2017, fig. 3). Note narrow, symmetrical, transversely extended thecal apertures projected on both sides into ear-like lateral processes ("horns" of earlier authors); B, E – distal thecae; C, D – proximal thecae.

also be seen in the uncompressed pyrite mould specimens of some of these taxa illustrated by Sudbury (1958; "*M. separatus separatus*" and "*M. separatus fimbriatus*" on pl. 19, "*M. separatus triangulatus*" on pl. 20).

The thecae terminate in relatively narrow, proximally facing apertures, transversely extended into a pair of slightly enrolled lateral processes the concave surfaces of which face proximally to dorso-proximally. This is well illustrated by rare chemically isolated fragments of *D*. ex gr. *triangulatus* from Arctic Canada (Fig. 4B–E). The considerable morphological variability observed in the thecal apertures of flattened specimens is most likely a combination of both primary biological variability and secondary taphonomical variation. In particular, the apertural parts of the thecae are variously deformed by differing degrees and angles of flattening. We presume that in the case of burial in relatively soft sediment, the thecae are likely to have been flattened in profile with lateral processes oriented perpendicular to the rhabdosome plane, buried within the under- and overlying soft sediment. In case of "cling-film preservation", in which the sediment surfaces are believed to have been firm due to bacterial mats (Jones *et al*. 2002), which appears to have been particularly common in Silurian graptolite black shales, the lateral apertural processes are commonly flattened and folded, either one up and one down over the aperture (Figs 7A, C, E; 8R; 9G, K), both folded up (Figs 6D, E; 7C; 8O), or both folded down (Figs 5G, 8L, 9K), or, in some cases the whole aperture was laterally twisted showing both processes extended in their original horizontal position (Figs 6C; 7E, J; 9B, D, E, P). The lateral apertural processes are usually small in the most proximal thecae and became more prominent in mesial and distal thecae as shown on Fig. 4B–E, for example.

The tightly curved proximal parts of *D. major*, *D. pectinatus* and stratigraphically high specimens of *D. triangulatus,* with the sicula and th1 crossing the stipe at the level of about th7, suggest that the rhabdosome had a low helical spiral shape that has been flattened onto a single plane by clingfilm preservation.

Systematic Palaeontology

The measurements of dorso-ventral width (DVW) and two-thecae repeat distance (2TRD) at several points along the rhabdosome for all described species are presented in Tab. 1.

Family Monograptidae Lapworth, 1873

Genus *Demirastrites* Eisel, 1912

Type species. – *Demirastrites triangulatus* Harkness, 1851, from Frenchland Burn near Moffat, Scotland. Subsequently designated by Přibyl & Münch (1942, p. 3).

Diagnosis. – (emended from Štorch 2015). Rhabdosome with proximally accentuated dorsal curvature. Sicula small. Thecae isolated, ventral prothecal wall free, parallel to rhabdosome axis, concave or slightly inclined. At least three or four proximal thecae rastritiform to sub-rastritiform, although th1 is commonly elongate. Distal thecae either sub-rastritiform or high-triangular. Thecal apertures proximally facing, slightly hooked, narrow, symmetrical, transversely extended into a pair of ear-like lateral apertural processes.

***Demirastrites campograptoides* sp. nov.**
Figures 5A–G; 6A, H

2015 *Demirastrites* sp. – Štorch, pp. 885, 886, figs 16c, 17e.
2018 *Demirastrites*? *raitzhainensis* (Eisel). – Štorch *et al*., p. 369, fig. 7j.

Holotype. – Specimen no. PŠ 3988a from the lower Aeronian middle *triangulatus* Biozone (sample HT160–170) of the Hlásná Třebaň section, Bohemia; figured by Štorch *et al*. (2018, p. 369, fig. 7j) and refigured herein in Fig. 5F.

Type horizon and locality. – Lower Aeronian middle *triangulatus* Biozone, sample HT160–170, Hlásná Třebaň section, Bohemia.

Material. – Ten flattened, more-or-less complete rhabdosomes from the middle–upper *triangulatus* and lowermost *pectinatus* biozones of Hlásná Třebaň section, and two incomplete specimens from Všeradice.

Etymology. – *Campograptoides*, after the distal thecae, which superficially resemble those of coeval species of the genus *Campograptus*.

Diagnosis. – Rhabdosome dorsally curved, hook-shaped in proximal part, 1.0–1.4 mm wide distally. Sicula small, apex attaining the level of the dorsal wall of the first metatheca. Thecae markedly biform. Nine to twelve proximal thecae sub-rastritiform. Distal thecae triangular, strongly inclined, numbering 9–10 in 10 mm, terminated by rounded weak hooks with narrow, proximally facing apertures transversely extended into relatively small lateral processes.

Description. – The rhabdosome is dorsally curved throughout, hook-shaped in the proximal part, which is curved through an angle of 180–270° within 10 proximal thecae. The sicula is 0.7–0.8 mm long, straight, and 0.16–

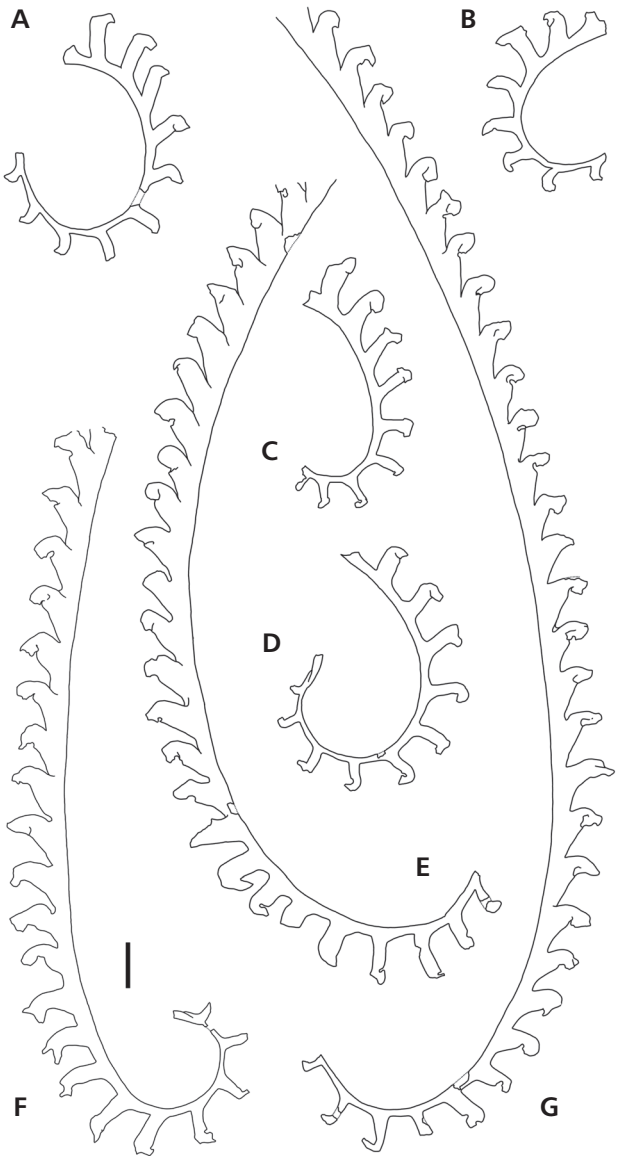

Figure 5. *Demirastrites campograptoides* sp. nov.; A – PŠ 4235, sample HT150–160; B – PŠ 4308, sample HT150–160; C – PŠ 4302, sample HT160–170; D – PŠ 4033, sample HT160–170; E – PŠ 3991, sample HT150–160; F – PŠ 3988a, holotype, sample HT160–170; G – PŠ 4155, sample HT170–180. All specimens from Hlásná Třebaň. All figures ×6, scale bar represents 1 mm.

Table 1. DVW and 2TRD measurements (in mm). Abbreviations: M – mean value; n – number of specimens; (s) – single specimen measured.

Species and form	DVW th1			DVW th2			DVW th3			DVW th4		
	range	M	n	range	M	n	range	M	n	range	M	n
D. triangulatus – early	0.3–0.5	0.38	24	0.35–0.75	0.55	27	0.55–0.95	0.72	30	0.65–1.1	0.81	19
D. triangulatus – typical										0.85–1.15	–	–
D. triangulatus – late	0.35–0.55	0.42	23	0.55–0.75	0.64	32	0.62–0.98	0.9	42	0.75–1.15	0.96	43
D. major – early	0.48 (s)	–	–	0.6–0.78	–	–	0.74–0.98	–	–	0.9–1.2	–	–
D. major – late	–	–	–	0.4–0.55	–	–	0.63–0.81	–	–	0.63–0.8	–	–
D. pectinatus – early	0.4–0.6	0.5	31	0.55–0.75	0.65	33	0.7–0.92	0.81	32	0.78–1.12	0.89	37
D. pectinatus – late												
D. campograptoides	0.35–0.55	–	–	0.5–0.65	–	–	0.6–0.85	–	–	0.75–1.0	0.86	10

Table 1. continued.

Species and form	DVW th5			DVW th10			DVW distal			2TRD th2		
	range	M	n	range	M	n	range	M	n	range	M	n
D. triangulatus – early	0.75–1.25	1.04	19	0.65–1.15	0.86	26	1.25–1.75	1.5	15	1.3–1.9	1.47	16
D. triangulatus – typical	1.0–1.4	1.14	11	1.3–2.0	1.65	53	1.5–1.8	1.65	13	1.35–2.2	–	–
D. triangulatus – late	0.9–1.3	1.1	41				1.3–2.0	1.64	40	0.9–1.6	1.15	33
D. major – early	0.7–1.4	–	–	1.4–2.05	1.66	13	1.4–2.05	1.66	13	1.4–1.6	–	–
D. major – late	0.6–1.3	–	–	1.05–2.2	1.5	10	1.05–2.2	1.49	10	2.15 (s)	–	–
D. pectinatus – early	0.9–1.15	1.01	41	1.3–1.7	1.48	12	1.56–1.9	–	–	0.75–1.3	0.9	10
D. pectinatus – late				1.15–1.65	1.38	31	1.45–1.8	1.62	23	0.7–1.2	0.82	22
D. campograptoides	0.8–1.1	0.92	10	0.75–1.0	0.86	10	1.0–1.4	–	–	1.2–1.6	–	–

Table 1. continued.

Species and form	2TRD th3			2TRD th5			2TRD th10			2TRD distal		
	range	M	n	range	M	n	range	M	n	range	M	n
D. triangulatus – early	1.05–1.65	1.34	20	1.3–1.9	1.49	20	1.8–2.1	1.96	13	2.0–2.55	2.18	11
D. triangulatus – typical	1.2–1.95	–	–	1.25–1.9	1.56	15	1.7–2.0	1.76	11	1.7–2.1	–	–
D. triangulatus – late	0.8–1.71	1.07	45	0.7–1.5	1.03	49	0.9–1.6	1.2	41	1.6–2.25	1.81	19
D. major – early	1.1–1.52	–	–	1.15–1.7	1.33	10	1.2–1.8	1.46	21	1.25–2.1	1.65	20
D. major – late	1.6–2.6	–	–	1.6–2.54	–	–						
D. pectinatus – early	0.7–1.25	0.89	10	0.6–1.2	0.91	46	0.9–1.5	1.2	39	1.5–2.2	1.85	28
D. pectinatus – late	0.6–1.0	0.78	29									
D. campograptoides	1.1–1.6	–	–	1.25–1.8	1.48	11	1.4–1.93	–	–	1.7–2.1	–	–

0.18 mm wide at the aperture. The apex of the sicula attains the level of the base of the dorsal metathecal wall of th1 or up to 0.2 mm below. The thecae are markedly biform. Nine to twelve proximal thecae are sub-rastritiform with slightly hooked apertures furnished with small lateral processes. The first theca, which possesses a tapering metatheca,

Figure 6. A, H – *Demirastrites campograptoides* sp. nov.; A – PŠ 3991, sample HT150–160; H – PŠ3988b, sample HT160–170. • B, C, J – *Demirastrites major* (Elles & Wood), late morphotype of the species; B – PŠ 4032, sample HT90–100; C – PŠ 4028, sample HT90–100, twisted sub-proximal thecae showing thecal apertures transversely extended into prominent lateral processes; J – PŠ 3925, sample HT90–100. • E – *Demirastrites major* (Elles & Wood), early morphotype, PŠ 4027, sample HT100–110. • D, G, I – *Demirastrites pectinatus* (Richter), late morphotype; D – PŠ 4200, sample HT120–130; G – PŠ 3996, sample HT110–120; I – PŠ 3992, sample HT110–120. • F – *Demirastrites pectinatus* (Richter), early morphotype; PŠ 4234, sample HT130–140. All specimens from Hlásná Třebaň. Figures A–B, D, F–I, ×5; figures C–E, J, ×10; scale bars represent 1 mm.

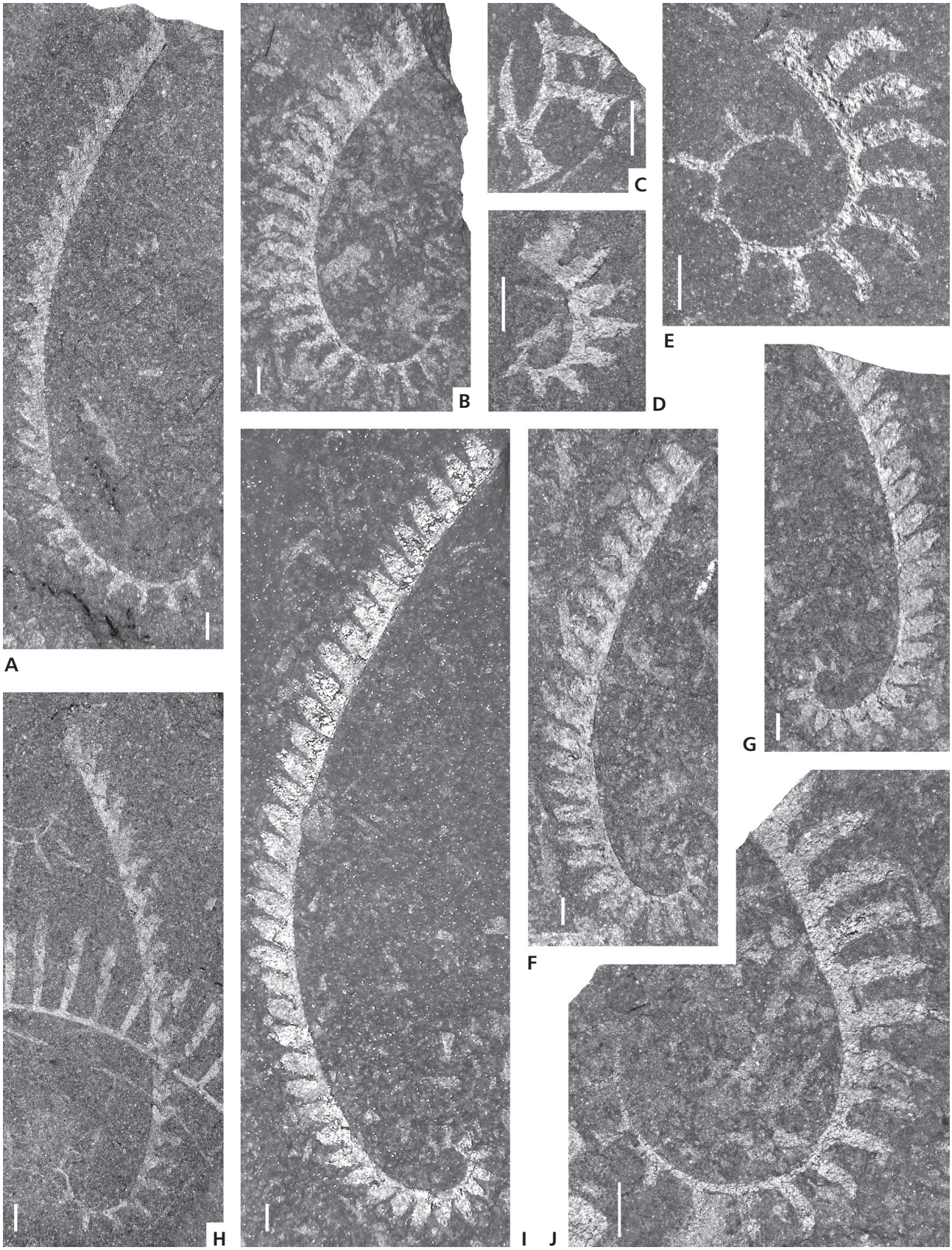
A
B
C
D
E
F
G
H
I
J

buds 0.2–0.35 mm above the sicular aperture. The prothecae are 0.4–0.7 mm long in the five most proximal thecae, and prothecal width increases from 0.08 mm at th2 to nearly 0.2 mm at th5. The proximal metathecae are slightly narrowing tubes *ca* 0.2 mm wide at th2 and 0.2–0.3 mm wide at th5, all inclined at a mean angle of 78°. Subsequent thecae become more inclined, more triangular, and more markedly hooked. Prothecal length decreases to 0.2–0.5 mm at th10, whereas prothecal width increases to 0.25–0.35 mm. Distal metathecae attain a mid-point width of 0.3–0.45 mm. Distal thecae are triangular with no distinct prothecal tube, inclined at 40–55° to the rhabdosomal axis, and terminated by rounded, weak hooks with proximally facing apertures and apparently short lateral apertural processes.

Discussion. – This uncommon species was assigned to *Demirastrites raitzhainensis* (Eisel) by Štorch *et al*. (2018) due to its relatively strongly inclined, blunt and rounded distal thecae, which are almost campograptid in shape. *Monograptus raitzhainensis* was named (as *Monograptus convolutus* var. *Raitzhainiensis*) but neither described nor figured by Eisel (1899) and was first figured but still not described by Eisel (1908). Close examination of the figures and description of the material subsequently described by Törnquist (1907) and Eisel (1912) reveals that the distinctive appearance of this form is a preservational artefact, with distal thecae heavily deformed by tectonic strain, a possiblity discussed by Törnqust (1907). In addition, specimens identified and figured as *M. raitzhainensis* by Elles & Wood (1913) were assigned to *M. separatus separatus* and *M. separatus triangulatus* by Sudbury (1958) and, therefore, to *Demirastrites triangulatus* in the sense of the present paper.

Demirastrites campograptoides is distinguished from other species of *Demirastrites* primarily by its more highly inclined distal thecae, lower distal DVW, and generally lower distal 2TRD. In addition, the lateral processes appear to be less prominent on the distal thecae of *D. campograptoides* compared with the other taxa described here, resulting in the appearance of simpler thecal hooks upon flattening. In contrast, the presence of both lateral thecal apertural processes and sub-rastritiform proximal thecae distinguish this species from species of *Campograptus*. In addition, species of *Campograptus* are generally characterized by metathecae that are relatively shorter compared to their width.

***Demirastrites major* (Elles & Wood, 1913)**
Figures 6B, C, E, J; 7A–L

1913 *Monograptus triangulatus* var. *major*, var. nov.; Elles & Wood, p. 472 (pars), pl. 47, fig. 5c (?5d, *non* 5a, b), text-fig. 328b (*non* 328a).
1958 *Monograptus separatus major* Elles & Wood. – Sudbury, p. 506, text-fig. 10.
? 1963 *Monograptus triangulatus* var. *major* E. & W. – Willefert, pp. 45, 46, pl. 2, fig. 2, text-fig. 73.
? 1967 *Demirastrites triangulatus major* (Elles & Wood). – Obut *et al*., p. 128, pl. 18, figs 3, 4.
1970 *Monograptus triangulatus major* Elles & Wood. – Rickards, p. 81, text-fig. 18-2.
1975 *Monograptus triangulatus major* Elles & Wood. – Hutt, pp. 110, 111, pl. 20, fig. 1.
non 1995 *Demirastrites triangulatus major* (Elles et Wood). – Li, p. 272, pl. 29, fig. 6.
2015 *Demirastrites major* (Elles & Wood). – Štorch, p. 885, figs 17r, 18e.
2018 *Demirastrites major* (Elles & Wood). – Štorch *et al*., p. 371, fig. 8c, o.

Lectotype. – Designated by Přibyl & Münch (1942, p. 7), new designation by Bulman (1957, p. 314), see also Sudbury (1958, p. 507). Specimen no. GSM26326 from the Rheidol Gorge, Wales, figured by Elles & Wood (1913, text-fig. 328b).

Material. – Twenty-nine flattened, more-or-less complete rhabdosomes from the lower and middle *pectinatus* Biozone of the Hlásná Třebaň section and four incomplete rhabdosomes from Všeradice.

Diagnosis. – Rhabdosome dorsally curved, coiled in the proximal part, attaining a width of 2.0–2.3 mm by th18–20. Proximal thecae slender, rastritiform to sub-rastritiform, commonly slightly ventrally curved. Distal thecae sub-rastritiform, parallel-sided, slightly ventrally curved, numbering 10–12 in 10 mm. Narrow, proximally facing thecal apertures transversely extended into prominent lateral processes.

Description. – The rhabdosome is arcuate, with dorsal curvature that is more tightly coiled and probably slightly helicoidal in the proximal part. It is curved through more than 300° within 10 proximal thecae, crossing the mesial part of the rhabdosome in the stratigraphically lowest specimens (early form) from the lower *pectinatus* Biozone. In stratigraphically higher specimens (late form), however, the proximal end is more protracted and less strongly coiled (Figs 6J; 7B, C, F). Mature rhabdosomes attain more than 30 mm in length. The sicula and th1 have not been identified with certainty in the present specimens. The most proximal preserved thecae (likely th2–th5) are slender and rastritiform to sub-rastritiform (slightly ventrally curved), and the prothecal tubes of the late form are of the same length or longer than the metathecae [0.6–1.2 mm at th3, 0.5–1.15 mm (M = 0.65 mm, n = 18) at th5]. The prothecal width varies between 0.1 and 0.2 mm at th5.

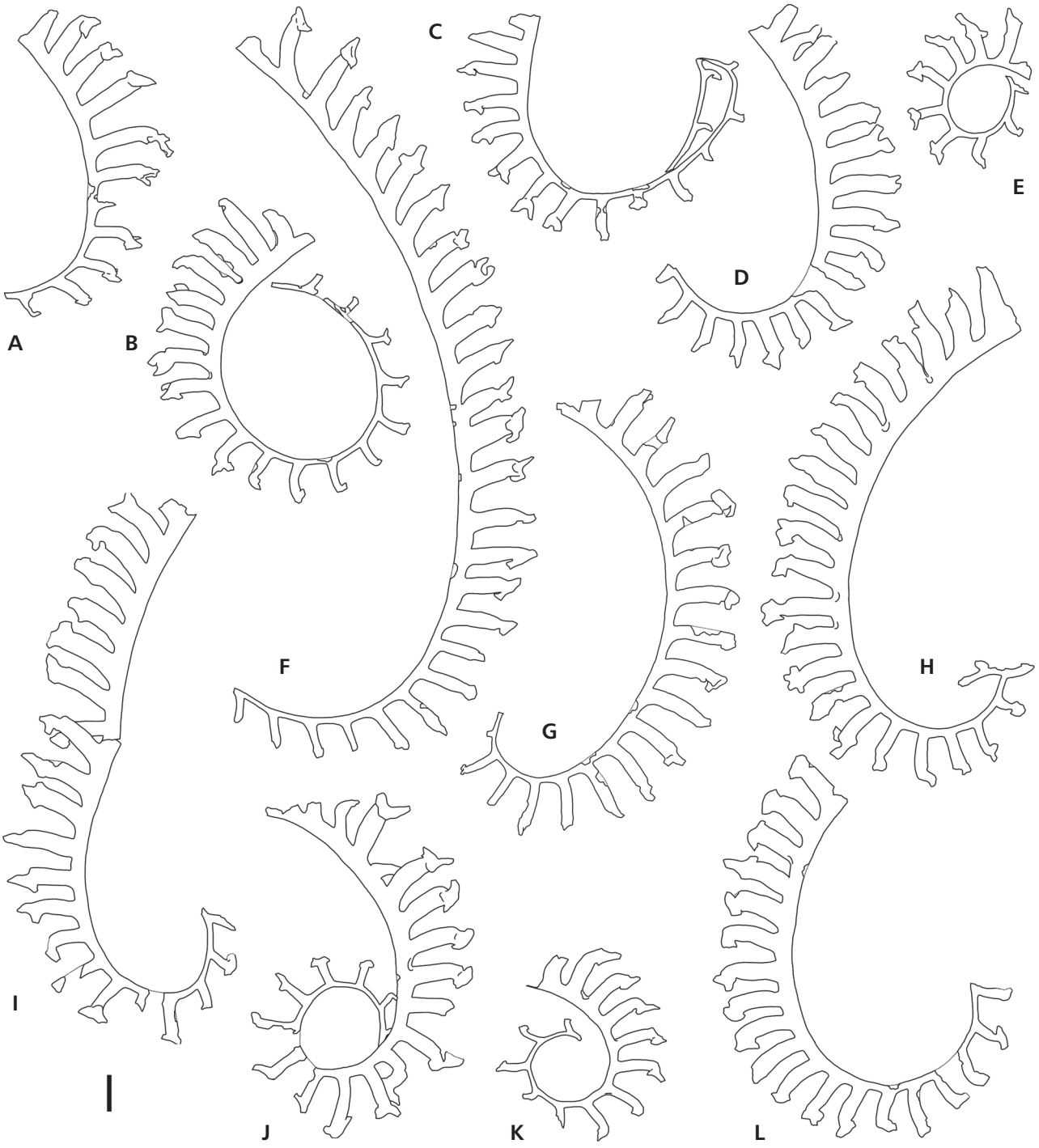

Figure 7. *Demirastrites major* (Elles & Wood); A – PŠ 4055, sample HT70–80; B – PŠ 4070, sample HT80–90; C – PŠ 4064, sample HT80–90; D – PŠ 4029, sample HT90–100; E – PŠ 4031, sample HT90–100; F – PŠ 4056, sample HT70–80; G – PŠ 4300; H – PŠ 4032, sample HT90–100; I – PŠ 4040, sample HT90–100; J – PŠ 4022, sample HT100–110; K – PŠ 4027, sample HT100–110; L – PŠ 4025, sample HT100–110. All specimens from Hlásná Třebaň except for G from the lowermost *pectinatus* Biozone of Všeradice. Figures A–C, F and ?G illustrate the late morphotype of the species; figures D–E, H–L exhibit the early morphotype. All figures ×6, scale bar represents 1 mm.

Metathecal tubes of the proximal thecae are straight or very slightly ventrally curved, *ca* 0.15 mm wide at th2 and 0.15–0.35 mm at th5, inclined at an angle of 50–75° at th2 and 65–90° at th5. Mesial thecae are more densely spaced, with 0.3–0.75 mm long and 0.15–0.3 mm wide prothecae. The parallel-sided, tubular metathecae are 1.2–2.2 mm (M = 1.6 mm, n = 23) high and 0.25–0.45 mm wide at th10 and are most commonly slightly ventrally curved. The

maximum DVW of the rhabdosome (Tab. 1) is attained by th18–20. Distal thecae most commonly possess short, 0.3–0.5 mm wide, distinct prothecal tubes, concave in ventral outline, and with high, generally parallel-sided to slightly tapering, ventrally curved metathecae that are 0.4–0.55 mm wide, and only slightly inclined (70–90°) to the rhabdosomal axis. The thecal apertures possess fully developed dorsal hoods furnished with a pair of lateral processes that are best seen when twisted into a facing profile (Figs 6C; 7E, J, L). The original position of the lateral apertural processes (described as lateral horns by some earlier authors) must have been approximately perpendicular to the axial plane of the theca. The lateral processes are small, *ca*. 0.2 mm long in the proximal thecae (up to th5), and became more prominent, 0.3–0.4 mm long, in the mesial and distal thecae. The most common preservation of the thecal apertures, however, exhibits just one visible lateral process folded across the dorsal margin of the apertural hood.

Discussion. – *Demirastrites major* can be distinguished from other species of *Demirastrites* by having generally parallel-sided, slightly ventrally curved metathecae distally, which are separated by short, distinct prothecal tubes. In addition, the distal DVW is more than 2.0 mm (normally 2.2 to 2.3 mm) beginning at about th18–20. The thecal apertures are furnished with particularly prominent lateral processes. The proximal part of the rhabdosome is rather protracted and less strongly coiled in the late form, with metathecae shorter and more widely spaced than those in other demirastritids of the *triangulatus* group. The early form of this species, which occurs in the lower *pectinatus* Biozone at Hlásná Třebaň (Figs 6E; 7E, J, K), possesses a generally shorter and more tightly coiled proximal part with shorter, less widely spaced thecae, resembling those of the stratigraphically highest forms of *D. triangulatus*. The same morphology has been found in specimens from Všeradice, which were also collected from the lower *pectinatus* Biozone. Specimens from higher parts of the *pectinatus* Biozone (Figs 6B, J; 7A–C, F) exhibit progressive straightening of the proximal part and further prothecal elongation, combined with shorter proximal metathecae, resulting in a more gradual distal increase in DVW.

Sudbury (1958) reported *D. major* as "fairly certain[ly]" from the *magnus* Band of the Rheidol Gorge section. The *magnus* Band at Rheidol Gorge occurs within the upper part of the range of "*Monograptus fimbriatus*" (= *D. pectinatus*) and, therefore, probably corresponds with the middle to upper part of the *pectinatus* Biozone as recognized in the Prague Synform.

"*Monograptus triangulatus* var. *major*", identified by Willefert (1963) from central Morocco, possesses long and relatively densely spaced thecae in its tightly enrolled proximal part. The figured specimen may be tentatively assigned to either the early form of *D. major* or the late form of *D. triangulatus* (see below). Specimens from the Kolyma Basin of northeastern Siberia, assigned to *D. triangulatus major* by Obut *et al*. (1967), possess a significantly wider rhabdosome, with a DVW of 3.0–3.5 mm attained 10 mm from the proximal end, and widely spaced distal thecae, which number 7–9 in 10 mm. Those specimens came from a single locality and appear to be affected by tectonic strain, so their identity is uncertain. The specimen identified as *Demirastrites triangulatus major* figured by Li (1995) from Yichang, China, is a distal fragment of *Lituigraptus* with typical, ventrally directed, wedge-shaped thecal apertural processes.

***Demirastrites pectinatus* (Richter, 1853)**
Figures 6D, F, G, I; 8A–R

1853 *Monograptus pectinatus*; Richter (pars), p. 461, pl. 12, fig. 26 (*non* 27).
1868 *Graptolites fimbriatus* n. sp. – Nicholson, p. 536, pl. 20, fig. 5, ?figs 3, 4.
1897 *Monograptus fimbriatus* Nich. – Perner (pars), pp. 28, 29, pl. 11, fig. 39, pl. 12, figs 13, ?18, pl. 13, figs 21–23 (*non* 25).
1899 *Monograptus fimbriatus* Nicholson. – Törnquist, p. 18, pl. 3, fig. 24.
1912 *Demirastrites pectinatus*, Richter. – Eisel (pars), p. 39, pl. 3, figs 16, 18–20 (*non* 17).
1913 *Monograptus fimbriatus* (Nicholson). – Elles & Wood (pars), p. 482, pl. 48, figs 4a, d (*non* b, c), text-figs 338a, b, ?(c, d).
1942 *Demirastrites pectinatus pectinatus* (Richter). – Přibyl & Münch, pp. 8, 9, pl. 1, fig. 6, text-fig. 1-4, 1-5.
1958 *Monograptus separatus fimbriatus* (Nicholson). – Sudbury, p. 499, pl. 19, figs 40–51, text-fig. 5.
1963 *Monograptus fimbriatus* (Nicholson). – Willefert, pp. 43, 44, pl. 2, fig. 1, text-fig. 69.
non 1968 *Demirastrites pectinatus pectinatus* (Richter). – Obut *et al*., p. 108, pl. 29, figs 4–6, pl. 30, figs 1, 2.
1970 *Monograptus triangulatus fimbriatus* (Nicholson). – Rickards, p. 82, pl. 7, fig. 4, text-fig. 17-2.
1971 *Monograptus (Demirastrites) pectinatus* (Richter). – Schauer, pp. 77, 78, pl. 26, fig. 1, pl. 27, fig. 1.
1975 *Monograptus triangulatus fimbriatus* (Nicholson). – Hutt, p. 110, pl. 20, fig. 5, pl. 21, figs 5, 6, pl. 22, figs 3, 4, 6, 7, text-fig. 17-6.
1975 *Monograptus pectinatus* Richter. – Bjerreskov, pp. 78, 79, pl. 11, fig. f, text-fig. 23d.
? 1982 *Monograptus triangulatus fimbriatus* (Nicholson). – Lenz, p. 116, figs 9l, m, q, 30b, g.
1989 *Monograptus pectinatus pectinatus* Richter. – Melchin, p. 1738, fig. 9x.
2003 *Demirastrites pectinatus* (Richter). – Loydell *et al*., p. 209, fig. 4r.

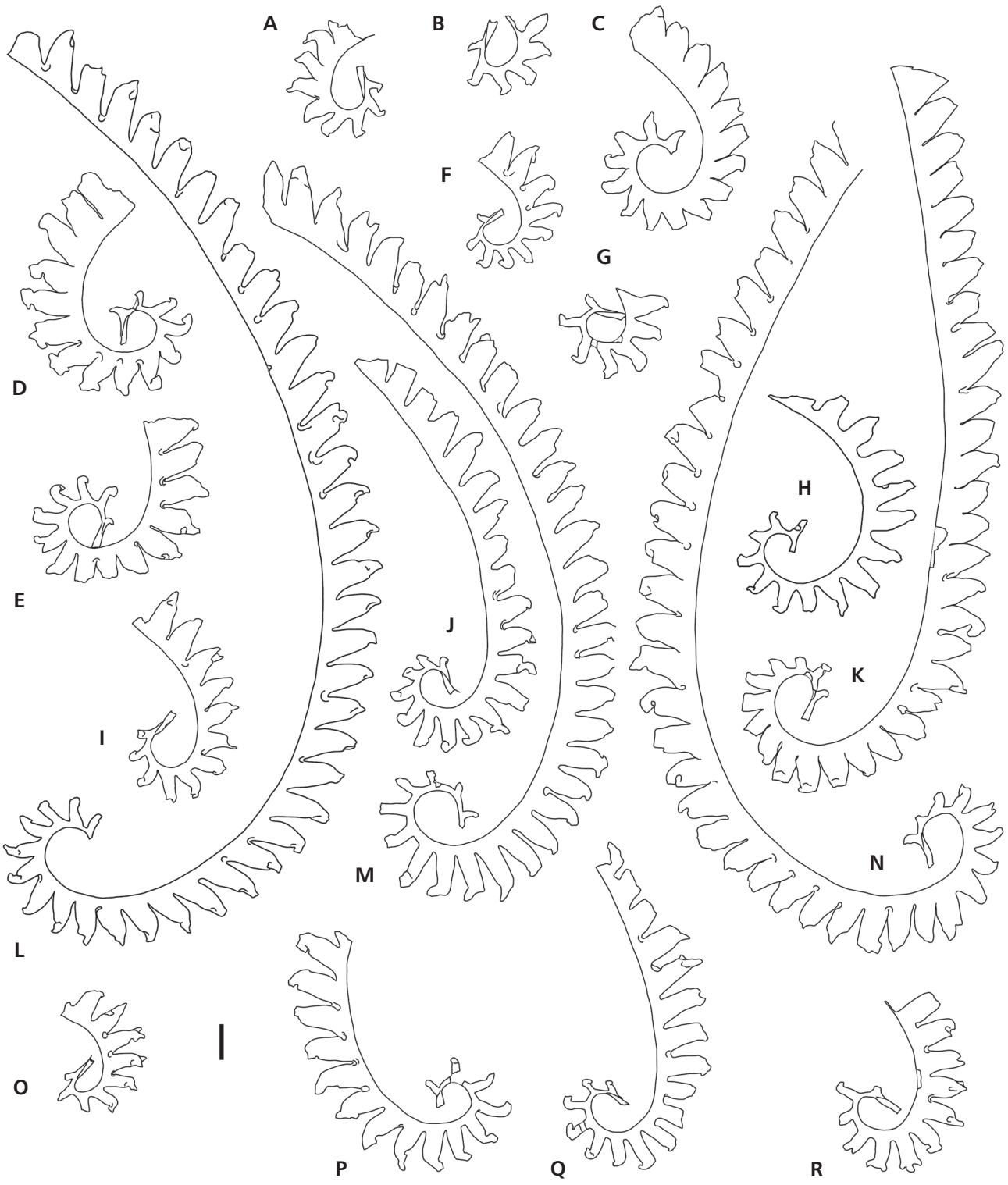

Figure 8. *Demirastrites pectinatus* (Richter); A – PŠ 4049, sample HT30–40; B – PŠ 4309, sample HT10–20; C – PŠ 4310, sample HT10–20; D – PŠ 4037, sample HT90–100; E – PŠ 4073, sample HT100–110; F – PŠ 4000, sample HT110–120; G – PŠ 4067b, sample HT80–90; H – ROM 45971, sample CM – 0–2, loose collection approximately equivalent to MCM2-98, 43–45 m, see Melchin *et al.* (2017, fig. 3); I – PŠ 4003, sample HT110–120; J – PŠ 4201, sample HT120–130; K – PŠ 4071, sample HT80–90; L – PŠ 4021, sample HT100–110; M – PŠ 4189, sample HT120–130; N – PŠ 4057, sample HT70–80; O – PŠ 4200, sample HT120–130; P – PŠ 3989, sample HT110–120; Q – PŠ 4195, sample HT120–130; R – PŠ 3997, sample HT110–120. All specimens from Hlásná Třebaň except for H from Cape Manning section, Cornwallis Island, Arctic Canada. Figures A–G, ?H, I, K–L and N–P represent the late morphotype of the species; figures J, M and Q, R represent the early morphotype. All figures ×6, scale bar represents 1 mm.

2009 *Demirastrites pectinatus*. – Piçarra *et al*., p. 46, fig. 5b.
2009 *Demirastrites pectinatus* (Richter). – Štorch & Kraft, p. 62, figs 7b, 8c, p. 68, 11j.
2017 *Demirastrites pectinatus* (Richter). – Loydell & Aung, p. 12, fig. 8g.
2017 *Demirastrites pectinatus* (Richter). – Loydell *et al*., p. 147, fig. 12j.
2018 *Demirastrites pectinatus* (Richter). – Štorch *et al*., p. 371, fig. 8k, p.
2018 *Monograptus triangulatus fimbriatus* (Nicholson). – Wilkinson, folio 3.32.

Holotype. – By monotypy. Specimen no. BGR X 10486 from Rothenbach bei Saalfeld, Thuringia, figured by Richter (1853, pl. 12, fig. 26).

Material. – Forty-eight flattened, mostly complete rhabdosomes from the *pectinatus* Biozone of the Hlásná Třebaň section and fourteen rhabdosomes from the Černošice section.

Diagnosis. – Rhabdosome with proximally accentuated dorsal curvature. Small sicula with apex attaining up to the level of the dorsal wall of the first metatheca. Three to rarely five proximal thecae sub-rastritiform, one or two somewhat axially elongated. Subsequent thecae become robust, bluntly triangular in outline. Metathecae weakly hooked, slightly more strongly hooked proximally, separated by a very narrow interspace or tightly appressed in flattened specimens. Narrow proximally facing thecal apertures furnished with short lateral processes.

Description. – The rhabdosome is strongly dorsally curved proximally, more weakly distally and the maximum length is at least 50 mm. The proximal dorsal curvature ranges from 255° to 340° (M = 298°, n = 25) within the first 10 thecae. The sicula is conical, short (0.7–1.0 mm), straight or gently ventrally curved, and 0.17–0.22 mm wide across its concave aperture, which possesses a short, narrow virgella. The sicular apex typically attains the level of the base of the dorsal metathecal wall of th1 or slightly (0.1 mm) below. The three or four (rarely five) most proximal thecae are sub-rastritiform and axially elongated, with short, slightly widening prothecal tubes and triangular metathecae, inclined at a relatively low mean angle of 71° at th2 (n = 32) and 79° at th5 (n = 44). The first theca is 0.75–1.0 mm long from its point of origin to the base of the dorsal wall of the metatheca. Its slender, 0.3–0.55 mm long protheca buds 0.15–0.4 mm above the sicular aperture. The protheca of th2 is 0.07–0.18 mm wide at its base, and subsequent prothecae widen through 0.15–0.32 mm at th5, and to 0.25–0.5 mm at th10. The metathecae are 0.17–0.4 mm wide at the mid-point of their height at th2, 0.3–0.48 mm at th5 and 0.5–0.75 mm at th10. Mesial and distal thecae become more robust and bluntly triangular in outline, inclined at a mean angle of 78° at th10 (n = 42) and 70° distally (n = 31). The distal thecae are 0.55–0.85 mm wide at the mid-point of their height. The prothecae are 0.3–0.6 mm wide and the prothecal tubes are entirely reduced in the mesial and distal thecae, leaving a very narrow interspace between the dorsal wall of one metatheca and the ventral wall of the subsequent metatheca. The thecae are weakly hooked, although slightly more strongly hooked proximally; the thecal apertures face proximally and are furnished with rather short (max. 0.2 mm) lateral processes that are commonly folded across the dorsal apertural hood to form a somewhat pointed termination of the generally triangular theca.

Discussion. – *Demirastrites pectinatus* (Richter, 1853) may be distinguished from most other triangulate monograptids by the fact that it possesses no rastritiform thecae and very few (usually four or less) sub-rastritiform thecae. Its most proximal thecae are axially elongated with triangular metathecae. The early form of *Demirastrites pectinatus* corresponds in thecal shape, DVW, thecal spacing and all other relevant characters to its junior synonym, *Monograptus triangulatus fimbriatus* (Nicholson, 1868), including the neotype of the latter species, which was designated by Sudbury (1958, p. 500). All specimens reported from the Yukon Territory, Canada (Lenz, 1982 and authors' collections) are small rhabdosomes with about 10 thecae or less, and the maximum dorso-ventral width of these rhabdosomes is only 1.3 mm, which is less than that measured at the corresponding theca in European populations or in those from Arctic Canada (Melchin 1989). In addition, the thecal spacing is closer (2TRD 1.1–1.35 mm, rarely up to 1.6 mm) and the angle of thecal inclination is also lower than that in European specimens. As a result the Yukon specimens are only questionably regarded as belonging to this species.

Regarding the form of the apertural processes, we speculate that these processes were laterally projected from both sides of the dorsal apertural hood based on details preserved in some flattened rhabdosomes (Fig. 8D, K, O, R). Somewhat more prominent dorsal apertural processes have been observed in early populations referred to *D. pectinatus*.

Demirastrites pectinatus can be readily distinguished from ?*Demirastrites similis* (Elles & Wood, 1913) by the more protracted proximal end of the former, which possesses a relatively low, triangular and axially elongated th1, and its sicula attains about the level of the first metatheca followed by several sub-rastritiform thecae. The proximal end of ?*D. similis* is more compressed in appearance, with a rather short and high th1 and a sicula

that attains the level of the metatheca of th2. In addition, ?*D. similis* appears to be lacking in sub-rastritiform proximal thecae after th1. As a result, we have only questionably placed that species in *Demirastrites*.

Specimens from the Norilsk Basin of western Siberia assigned to *D. pectinatus pectinatus* by Obut *et al*. (1968) attain a lesser maximum width (1.2–1.4 mm), and possess more broadly triangular thecae of almost campograptid appearance, inclined at 45° to the rhabdosome and terminated by apertural hooks composed, for the most part, of the dorsal thecal wall. Thecal apertures face proximally and probably lack the typical transversal extension into lateral processes. Proximal thecae are axially elongated and low-triangular in profile. Specimens have been reported from the lower part of the *triangulatus* Biozone, which contrasts with the range of *D. pectinatus* in European sections. These Siberian specimens closely resemble material assigned to *Demirastrites* cf. *triangulatus* by Chen (1984) from southern Shaanxi and southern Sichuan provinces in China and specimens collected by the present authors from the "*triangulatus* Biozone" of the Yuxian section in southeastern Sichuan.

***Demirastrites triangulatus* (Harkness, 1851)**
Figures 9A–X; 10A–I; 11

1851 *Rastrites triangulatus*; Harkness (pars), p. 59, fig. 3a, b (*non* c, d).
1897 *Monograptus triangulatus* Harkn. – Perner, p. 27, pl. 12, fig. 16, (?fig. 30), text-fig. 12.
1899 *Monograptus triangulatus* Harkness, var. *Raitzhainiensis* Eisel, p. 7. [*nomen nudum*]
1899 *Monograptus triangulatus* Harkness. – Törnquist, pp. 19, 20, pl. 3, figs 25–28, pl. 4, figs 1, 2.
1907 *Monograptus triangulatus* Harkness, var. *Raitzhainiensis* Eisel. – Törnquist, p. 17, pl. 3, figs 2–4.
1908 *Monograptus triangulatus* var. *Raitzhainiensis*. – Eisel, p. 220, fig. 11.
1912 *Demirastrites triangulatus*, Harkness. – Eisel, pp. 36, 37, pl. 3, figs 8–12, 14, 15, ?(6, 7, 13).
1913 *Monograptus triangulatus* (Harkness). – Elles & Wood (pars), p. 471, pl. 47, figs 4a, c, d (*non* b, e), text-fig. 327b (*non* a, c).
1913 *Monograptus raitzhainiensis* (Eisel). – Elles & Wood (pars), pp. 473, 474, pl. 48, fig. 3a (*non* b, c), text-fig. 329a (*non* 329b).
1942 *Demirastrites triangulatus* (Harkness). – Přibyl & Münch (pars), p. 3, pl. 1, figs 1–5, text-fig. 1-1, 1-2, (*non* 1-3).
1958 *Monograptus separatus triangulatu*s (Harkness). – Sudbury, pp. 503–506, pl. 20, figs 52–63 (see for further synonymy).
1958 *Monograptus separatus separatus* var. nov. – Sudbury, pp. 496–499, pl. 19, figs 33–39.
1963 *Monograptus triangulatus* (Harkness). – Willefert, p. 45, pl. 2, fig. 5, text-fig. 72.
? 1963 *Monograptus triangulatus* var. *major* E. & W. – Willefert, pp. 45, 46, pl. 2, fig. 2, text-fig. 73.
? 1965 *Demirastrites triangulatus* (Harkness). – Obut *et al*., pp. 86, 87, pl. 17, figs 1–3.
? 1968 *Demirastrites triangulatus triangulatus* (Harkness). – Obut *et al*., pp. 106–108, pl. 27, figs 3–5, pl. 28, figs 1–5, pl. 29, figs 1–3.
1970 *Monograptus triangulatus triangulatus* (Harkness). – Rickards, pp. 80, 81, text-fig. 18-1.
1970 *Monograptus triangulatus separatus* Sudbury. – Rickards (pars), p. 81, text-fig. 13-17, text-fig. 17-4 (*non* 17-3).
1971 *Monograptus* (*Demirastrites*) *triangulatus* (Harkness). – Schauer, p. 78, pl. 26, figs 9–11, pl. 27, fig. 3.
1975 *Monograptus triangulatus triangulatus* (Harkness). – Hutt, pp. 109, 110, pl. 19, figs 1, 2, pl. 20, figs 2, 7.
1975 *Monograptus triangulatus separatus* Sudbury. – Hutt, p. 111, pl. 21, fig. 1.
1975 *Monograptus triangulatus triangulatus* (Harkness). – Bjerreskov, pp. 77, 78, text-fig. 23a, pl. 11, fig. e.
? 1978 *Demirastrites triangulatus* (Harkness). – Chen & Lin, pp. 65, 66, pl. 15, figs 5–8, text-fig. 17b.
? 1982 *Demirastrites triangulatus* (Harkness). – Anhui Geological Survey Team, p. 114, pl. 28, figs 9, 10.
? 1995 *Demirastrites triangulatus* (Harkness). – Li (pars), p. 271, pl. 29, fig. ?5 (*non* 3, 4).
2000 *Monograptus triangulatus separatus* Sudbury. – Sudbury & Hutt, folio 1.64.
2003 "*Demirastrites*" *triangulatus* (Harkness). – Loydell *et al*., p. 209, fig. 4h.
2007 *Monograptus triangulatus triangulatus* (Harkness). – Zalasiewicz, folio 2.92.
2009 *Demirastrites triangulatus*. – Piçarra *et al*., p. 46, fig. 5a.
2015 *Demirastrites triangulatus* (Harkness). – Štorch, pp. 884, 885, figs 16a, b, 17f, h, m, n, 18b, c.
2017 *Demirastrites triangulatus* (Harkness). – Loydell & Aung, p. 13, fig. 9e.
2017 *Demirastrites triangulatus* (Harkness). – Loydell *et al*., p. 151, fig. 14h.
2018 *Demirastrites triangulatus* (Harkness). – Štorch *et al*., p. 367, fig. 6, p. 369, fig. 7l–n.

Lectotype. – Designated by Přibyl & Münch (1942, p. 4). Specimen no. GSM6941 from Frenchland Burn, Dumfriesshire, Scotland, figured by Harkness (1851, pl. 1, fig. 3a, ?b).

Material. – One hundred and nineteen flattened, more-or-less complete measured rhabdosomes from the *triangulatus* Biozone and lowermost *pectinatus* Biozone of the Hlásná Třebaň section and twelve rhabdosomes from Všeradice,

eight rhabdosomes from Karlík, ten rhabdosomes from El Pintado (Spain), and minor supplementary material from the Estana section (Spanish Pyrenees) and the Oberbuchach section (Carnic Alps).

Diagnosis. – Rhabdosome arcuate in distal part, hook-shaped to dorsally coiled in proximal part. Distal rhabdosome width ranges commonly from 1.5–1.65 mm, rarely 1.3 mm to 2.0 mm. Proximal thecae rastritiform to sub-rastritiform, first one or two thecae axially elongated. Distal thecae, numbering 9–11 in 10 mm, are either sub-rastritiform or, more commonly, high-triangular, but always separated by significant interspaces. Thecae terminated by proximally facing apertures transversely extended into a pair of lateral processes.

Description. – The present specimens of *D. triangulatus* show significant morphological changes in several characters between the lowest collections at the base of the *triangulatus* Biozone to the stratigraphically highest specimens from the lowermost *pectinatus* Biozone. Based on these variations in form we recognize three distinct morphotypes: the early form (ranges from HT200–207 to HT185–190 m); the typical form (which most closely resembles specimens assigned to this species in other parts of Europe and ranges from HT190–200 to HT170–180 m); and the late form (ranges from HT170–180 to HT120–130 m). Rhabdosomes from the lower part of the *triangulatus* Biozone, including both the early form and the typical form, are hook-shaped, tightly dorsally curved in the proximal part and moderately arcuate distally. The proximal end is curved through 250–300° (exceptionally 340°) up to the level of th10. The proximal end, which may have been helical in form, is more tightly coiled in the late forms, curving through a mean angle of 340° (n = 27) between th1 and th10.

The sicula is 0.75–1.05 mm long, 0.16–0.23 mm wide at the aperture, with its apex attaining 0–0.5 mm below the level of dorsal wall of the first metatheca. In the late form the sicula tends to be slightly shorter but its apex attains a relatively higher level relative to th1. In the early and typical forms the first two proximal thecae are axially elongated with, on average, relatively shorter and more inclined metathecae, than in the late form, which normally shows only one axially elongate theca proximally.

In the early form, all or most of the thecae from th3 onward are sub-rastritiform, with a distinct, widening prothecal tube and straight to slightly ventrally curved, weakly tapering metathecae. Only a few specimens possess distal thecae that are high-triangulate (*e.g.* Figs 9V, 10A).

In the typical form and late form nine to at least 15 proximal thecae (after th1) are rastritiform to sub-rastritiform, with significant interspaces between the normally straight metathecal tubes. In some specimens in the highest sample (HT120–130), however, the number of rastritiform to sub-rastritiform proximal thecae decreases to less than nine. Distal thecae in the typical form and late form are high-triangulate.

In the proximal to mesial thecae, the prothecae are slender, isolated tubes, 0.07–0.13 mm wide at th2, 0.1–0.23 mm at th5, 0.15–0.35 mm at th10 and 0.25–0.5 mm in distal thecae. Prothecal width usually increases towards the metatheca inflection point. On average, prothecal tube widths tend to be in the relatively narrower ends of this range of values in the early form and in the wider end of the range in the late form. Prothecal tubes in the early form and typical form are 0.3–0.8 mm long at th3 (M = 0.52 mm, n = 28), 0.3–0.75 mm at th5 (M = 0.49 mm, n = 35) at th5 and 0.25–0.55 mm at th10 (M = 0.41 mm, n = 24). Specimens of the late form are marked by more dense thecal spacing (see Tab. 1) and consequently lower prothecal tube length: 0.3–0.7 mm at th3 (M = 0.45 mm, n = 47), 0.15–0.5 mm at th5 (M = 0.34 mm, n = 52), and 0.21 mm (n = 44) at th10.

The metathecal tubes are generally straight, although they are sometimes ventrally curved in the early form. They widen from 0.12–0.25 mm at the mid-point of th2 (M = 0.18 mm, n = 31), to 0.2–0.35 mm at th5 (M = 0.26 mm, n = 81), 0.35–0.5 mm at th10 (M = 0.42 mm, n = 68), and 0.45–0.6 mm in distal thecae. Specimens of the late form exhibit slightly wider (0.5–0.65 mm) metathecal tubes in the distal part of mature rhabdosomes. The metathecae are terminated by proximally facing apertures that are transversely extended into a pair of lateral processes. These lateral processes, particularly prominent in specimens of the late form, are 0.1–0.3 mm long in proximal thecae and commonly up to 0.4 mm long in mesial and distal thecae (Fig. 9B, D, E, P).

The angle of inclination of the metathecal tubes increases from 57° at th2 (n = 29) in the early and typical

Figure 9. *Demirastrites triangulatus* (Harkness); A – PŠ 4192, sample HT120–130; B – PŠ 4231, sample HT130–140; C – PŠ 4042, sample HT140–150; D – PŠ 4233, sample HT130–140; E – PŠ 4039, sample HT140–150; F – PŠ 4107, sample HT120–130; G – PŠ 4237/2, sample HT130–140; H – PŠ 4271, sample HT170–180; I – PŠ 4248, sample HT185–190; J – PŠ 4268, sample HT180–185; K – PŠ 4043, sample HT140–150; L – PŠ 3990, sample HT160–170; M – PŠ 4249, sample HT185–190; N – PŠ 4214, sample HT150–160; O – SM. A24849, horizon S by Sudbury (1958); P – PŠ 4058, sample HT200–205; Q – PŠ 4269, sample HT195–200; R – MGM9201-O, sample EP440–460; S – PŠ 4246, sample HT180–185; T – PŠ 4301; U – PŠ 4276, sample HT195–200; V – PŠ 4224, sample HT200–205; W – PŠ 3927, sample HT205–207; X – PŠ 4228, sample HT190–195. All specimens from Hlásná Třebaň except for O from the Rheidol Gorge section, Wales; R from the El Pintado reservoir section, Spain and T from Všeradice. Figures A–H, K, L, and N represent the late morphotype of the species; figures M, I, J and R–T belong to the typical morphotype and figures O–Q and U–X represent the early morphotype. All figures ×6, scale bar represents 1 mm, crossed bars in figures O and R indicate tectonic strain.

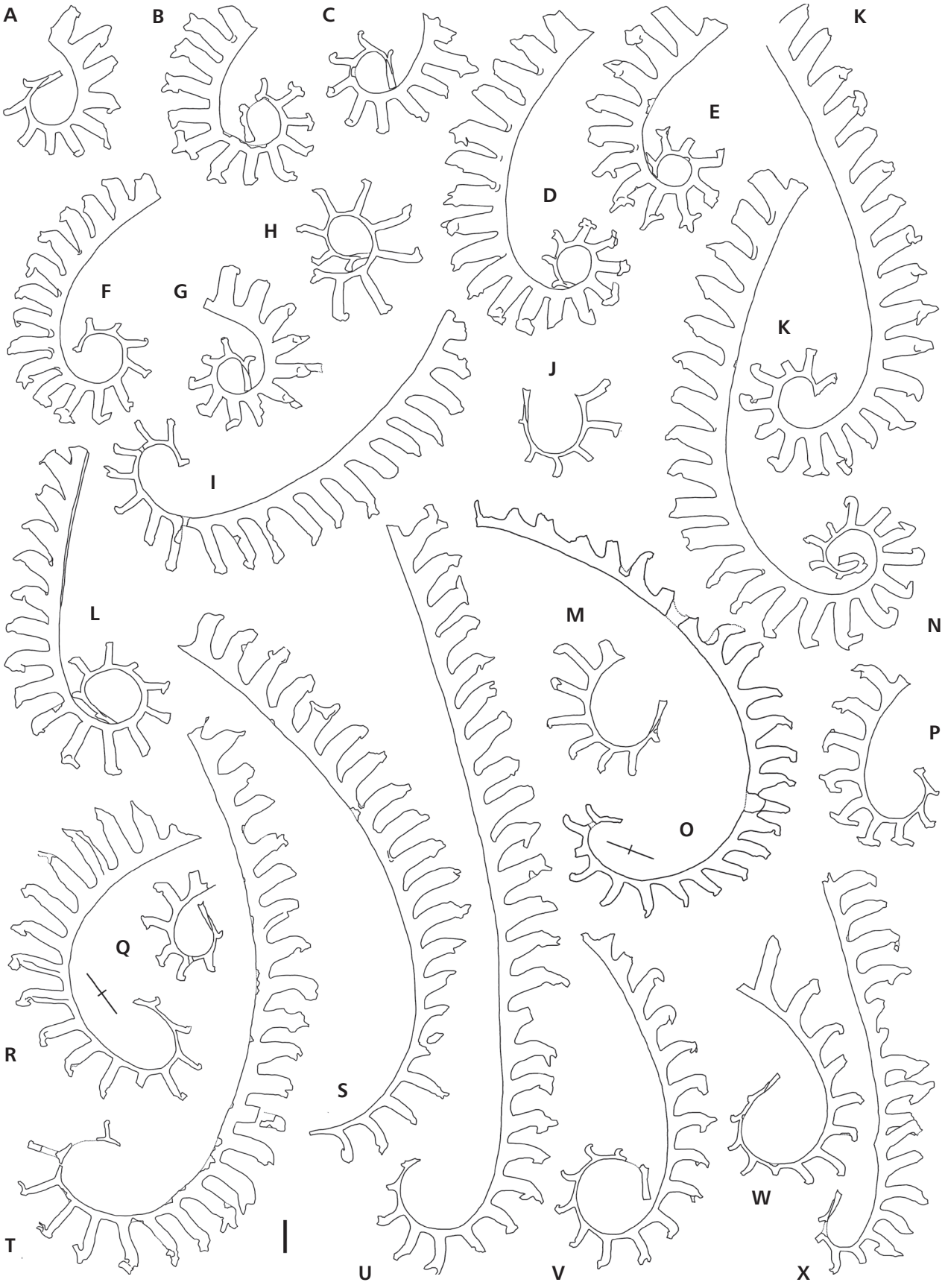
A
B
C
D
E
K
H
F
G
K
J
I
L
M
N
P
O
Q
R
S
T
U
V
W
X

forms, through 79° (n = 33) at th5, reaching the maximum of 81° at about th10 (n = 26) and decreases again to 73° (n = 15) in distal thecae. Specimens of the late form exhibit slightly, but consistently higher angles of metathecal inclination: M = 70° (n = 35) at th2, M = 83° (n = 49) at th5, M = 84° (n = 43) at th10 and 77° in the distal part of the rhabdosome.

Discussion. – *Monograptus triangulatus separatus*, described by Sudbury (1958, as *Monograptus separatus separatus,* but renamed as *M. triangulatus separatus* by Sudbury, 1959), based on specimens preserved as internal pyrite moulds from the Rheidol Gorge, was distinguished from *Monograptus triangulatus triangulatus* by having a slightly lower number of widely separated, rastritiform to sub-rastrititform proximal metathecae and a more gradual increase in DVW. Sudbury found that specimens assigned to *Monograptus triangulatus separatus* and *Monograptus triangulatus triangulatus* occurred together in many of the samples in the Rheidol Gorge succession, which suggests that they are not likely to represent either geographical or chronological subspecies of the same species. We have observed that the increase in DVW of the proximal part of the rhabdosome varies considerably in *D. triangulatus*. Specimens with DVW values similar to Sudbury's definition of *M. triangulatus separatus* occur in the lowermost *triangulatus* Biozone in the Prague Synform (*D. triangulatus* early form). *M. triangulatus separatus* was reported from a broad interval beginning at the base of the *triangulatus* Biozone up to the *magnus* Biozone in the Rheidol Gorge. A specimen that Sudbury had identified as *M. triangulatus separatus* from the base of the *triangulatus* Biozone is illustrated here (Fig. 9O), showing its close similarity to our *D. triangulatus* early form. However, the type specimen of *M. triangulatus separatus* came from Sudbury's horizon D, which we correlate with lower *pectinatus* Biozone of continental Europe due to its co-occurrence with *D. pectinatus* (= *M. triangulatus fimbriatus*) and other age-diagnostic taxa. Several of our stratigraphically higher specimens of *D. triangulatus* (late form) also show a reduced number of rastritiform to sub-rastritiform thecae (*e.g.* Fig. 9A, G), indicating that this character is also quite variable within this species. In addition, specimens of *D. pectinatus* with a small number of sub-rastritiform thecae occur in the lowest part of the *pectinatus* Biozone in the Hlásná Třebaň section. It is difficult to compare precisely the number of rastritiform to sub-rastritiform thecae in flattened specimens with those in three dimensional pyrite internal moulds from the Rheidol Gorge due to variation in the mode of flattening, combined with apparent primary morphological variability. We conclude, therefore, that *Demirastrites triangulatus separatus* falls well within the variability observed in populations of *D. triangulatus* and we see no basis for distinguishing the "*separatus*" form as a distinct subspecies.

Demirastrites extremus (Elles &Wood) can be easily distinguished from *Demirastrites triangulatus* by having approximately 12 widely spaced rastritiform thecae and a maximum DVW of 2.0–2.5 mm, which is attained between th9 and th12 before it gradually decreases to 1.8-2.0 mm in the distal part of the rhabdosome. As a result, we feel that it is sufficiently distinct from *D. triangulatus* to be regarded as a distinct species, rather than as a subspecies of the latter.

Based on the figured specimens (pl. 20, figs 64–66) and diagnosis provided by Sudbury (1958*), Demirastrites predecipiens* can be distinguished by its more axially elongated proximal thecae and lesser (1.2–1.4 mm) and more gradually increasing DVW. The widely separated proximal thecae, reported as rastritiform by Sudbury, appear sub-rastritiform on the figured specimens. The true status of this form will have to be re-examined based on its type collection supplemented by additional material.

Monograptus triangulatus var. *Raitzhainiensis* was recognized by Eisel (1899) and later described by Törnquist (1907) and Eisel (1908), based on flattened material that was heavily deformed by tectonic strain, which created the appearance of its short and broad, beak-like distal thecae. The validity of this form was questioned by Törnquist (1907), and the lectotype, designated by Přibyl & Münch (1942), is missing. Based on the published illustrations and descriptions we consider that the original material on which this species is based most likely represents tectonically deformed specimens of *D. triangulatus*.

Demirastrites triangulatus has been considered to be one of the most cosmopolitan species of the Llandovery graptolite fauna. However, we have closely examined specimens assigned to *D. triangulatus* in China and Siberia and have found significant differences from the material assigned to this species in Europe. The maximum distal width of Chinese and Russian specimens is only 1.5 mm with mean DVW values of 1.2–1.3 mm. Their metathecae are more triangular (less parallel-sided), and more widely spaced in the proximal part, separated by wider interspaces throughout the rhabdosome. The apertural hooks are more rounded and lateral apertural processes appear to be shorter. The prothecae commonly widen more toward the base of the metatheca. The dorsal curvature of the rhabdosome is less accentuated proximally in the Chinese and Siberian specimens and the proximal end possesses a slightly ventrally curved, rather than straight, sicula. The Chinese and Russian material may represent a different, although closely related species, although, conversely, they could represent a geographical subspecies of *D. triangulatus*. For this reason, we regard the synonymy of the Chinese and Russian material with *D. triangulatus* as questionable, pending detailed comparative morphometric study.

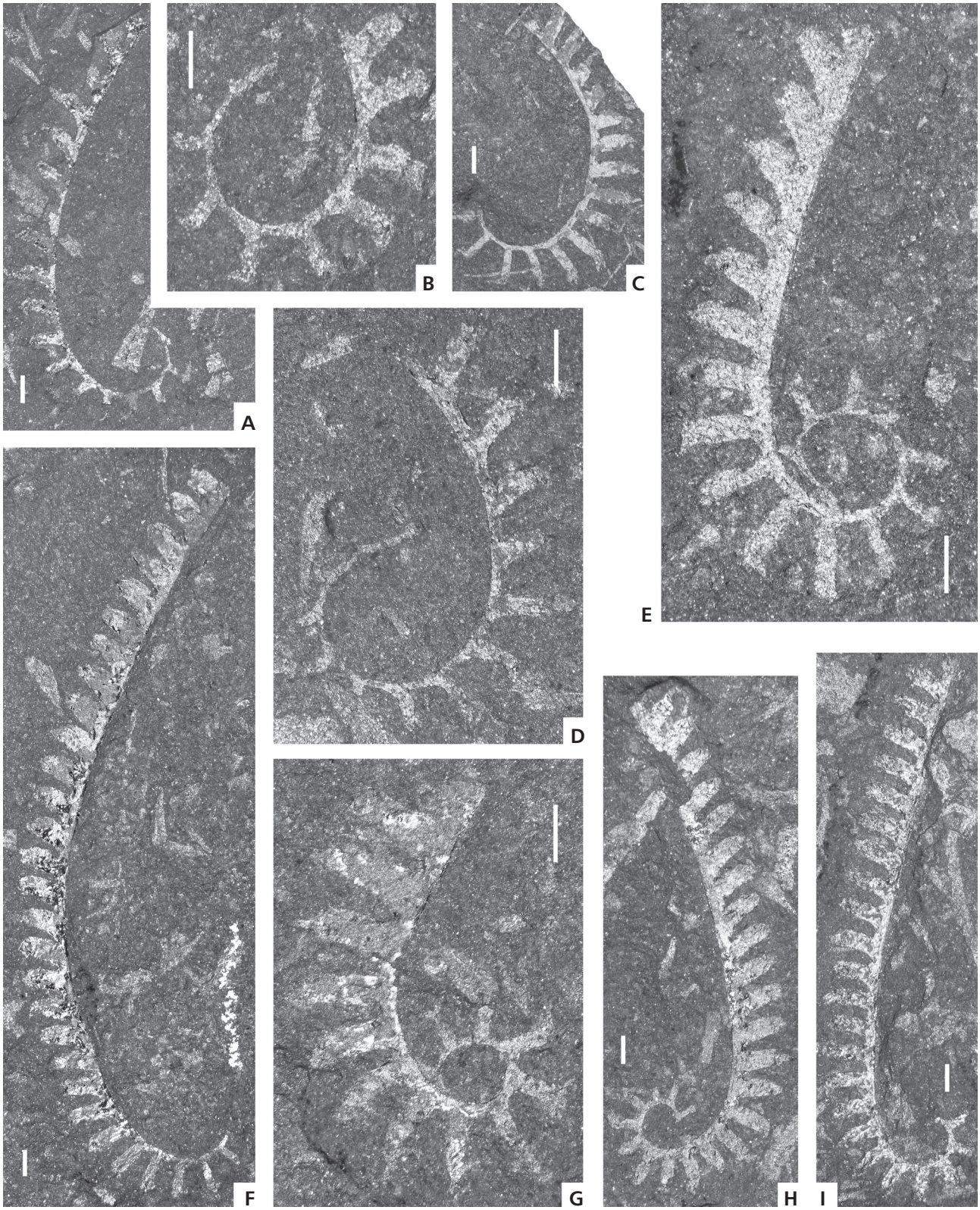

Figure 10. *Demirastrites triangulatus* (Harkness). • A, D – early morphotype of the species; A – PŠ 4310, sample HT205 – 207; D – PŠ 4304, sample HT205–207. • B, C, F, I – typical morphotype; B – PŠ 4267, sample HT185–190; C – PŠ 4216, sample HT195–200; F – PŠ 4210, sample HT180–185; I – PŠ 4244, sample HT190–195. • E, G, H – late morphotype; E – PŠ 3990, sample HT160–170; G – PŠ 4039, sample HT140–150; H – PŠ 4043, sample HT140–150. All specimens from Hlásná Třebaň. Figures A, C, F, H–I, ×5; figures B, D, E, G, ×10; scale bars represent 1 mm.

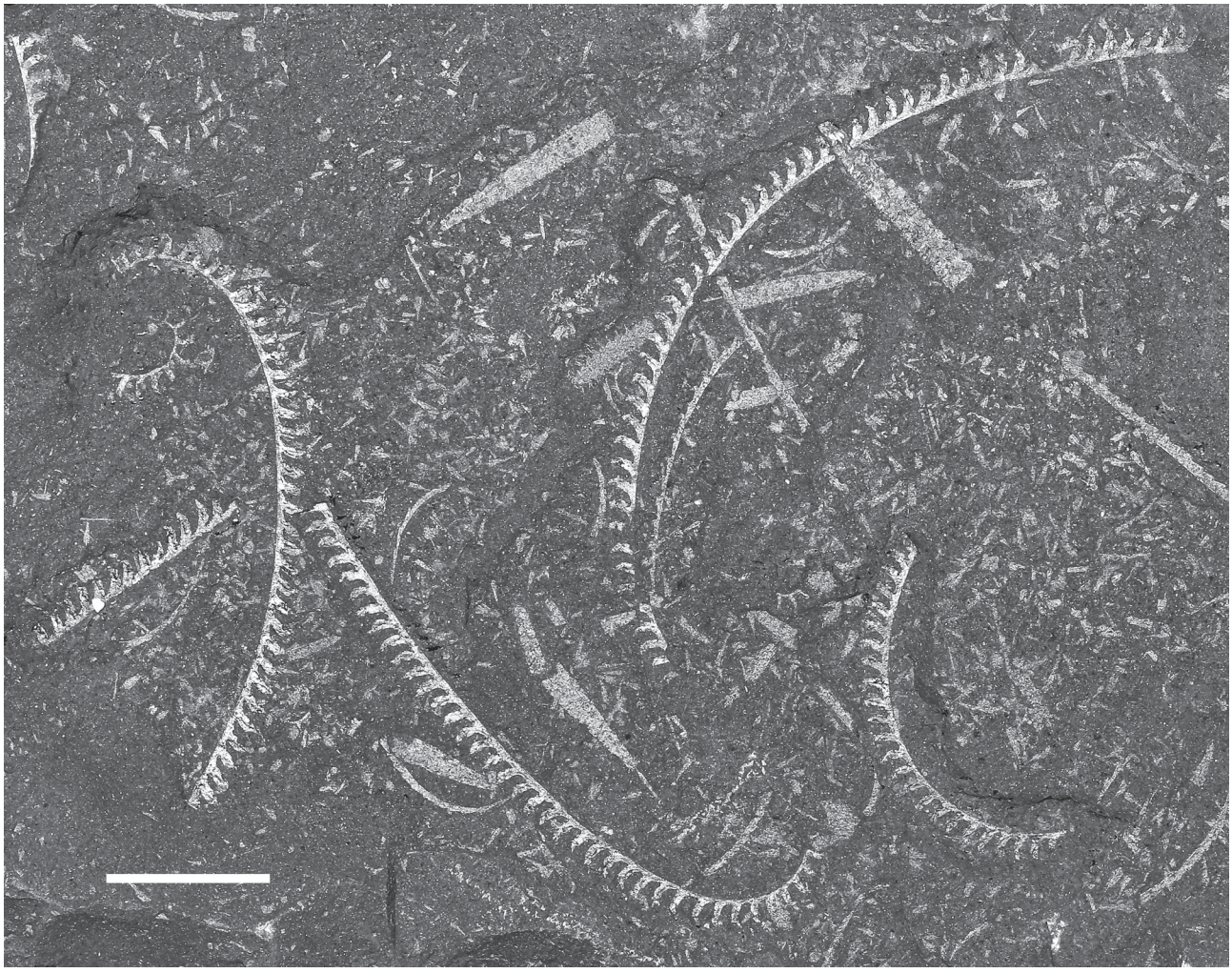

Figure 11. *Demirastrites triangulatus* (Harkness), early morphotype of the species; PŠ 4281, Hlásná Třebaň, sample HT190–195. Scale bar represents 10 mm.

Morphological changes, anagenesis, and speciation

Large collections of specimens of *Demirastrites* derived from bed-by-bed sampling of the lower Aeronian succession in the Prague Synform, supplemented by specimens from other localities in peri-Gondwanan Europe, have made it possible to document both gradual morphological changes within species and also patterns of apparent species divergence, which are shown in Fig. 2.

As noted above, populations of *Demirastrites triangulatus* can be divided into three distinct morphotypes. The early form (Figs 9O–Q, U–X; 10A, D; 11) is confined to the lowermost 22 cm of the species' range at Hlásná Třebaň (Fig. 2). It is common in four samples (HT200–207, HT195–200, HT190–195 and HT185–190). Within the relatively short range of the early form there appears to be a distinct trend toward increasing distal DVW and also greater mesial and distal metathecal width in higher collections (Fig. 12B, C). A second, slightly different morphotype (Figs 9M, I, J, R–T; 10B, C, F, I) co-occurs with the early form in samples HT195–200 and 185–190, and also occurs in the overlying sample, HT180–185. Despite its relatively short range at Hlásná Třebaň, we refer to this as the typical form because it most closely resembles specimens identified as this species in other studies of European material. Although there is significant overlap in the morphologies of the early form and the typical form, the early form differs from the typical form in the following respects: the DVW increases more slowly in the early form, which is particularly evident in its lower mean DVW at th10 (Tab. 1); the metathecae are commonly slightly ventrally curved in the early form, which is rare in the typical form (Fig. 9); distal 2TRD is generally higher in the early form (Tab. 1); the early form commonly retains sub-rastritiform thecae throughout the length of the rhabdosome, which is rare in the typical form; the typical form commonly shows several fully rastritiform thecae

in the proximal end, which are not seen in the early form. There are no evident morphological changes within the typical form through its range.

The third morphotype of *D. triangulatus* is the late form (Figs 9A–H, K, L, N; 10E, G, H), which occurs in all samples from HT170–180 (the sample above the highest occurrence of the typical form) to HT120–130, in the lower part of the *pectinatus* Biozone (Fig. 2). Its most conspicuous difference from the early and typical forms is that the late form shows a significantly more tightly coiled rhabdosome through the first ten thecae. The late form also differs from the typical form in that it possesses, on average, more closely spaced and less inclined thecae, as well as commonly showing more strongly developed lateral processes. As in the typical form, several of the proximal thecae are fully rastritiform in the late form. The late form of *D. triangulatus* shows a clear pattern of gradual morphological change in its proximal thecal spacing, with the 2TRD decreasing through its range (Fig. 12A). In addition, the stratigraphically highest specimens tend to have a lower number of rastritiform to sub-rastritiform thecae.

Two distinct forms are recognizable among specimens of *Demirastrites pectinatus* (Fig. 2). The early form (Figs 6F; 8J, M, Q–R) is restricted in its stratigraphical range to the HT130–140, HT120–130 and HT110–120 samples and overlaps in the lower two samples with late form of *D. triangulatus*. The early form of *D. pectinatus* closely resembles the late form of *D. triangulatus* in several respects, particularly in that they retain 4–5 sub-rastritiform thecae in the proximal end. On the other hand, the early form of *D. pectinatus* differs from the late form of *D. triangulatus* in the following respects (Fig. 2): loss of fully rastritiform proximal thecae and fewer sub-rastritiform proximal thecae; a more weakly coiled proximal part of the rhabdosome; less pronounced lateral apertural processes; lower 2TRD values, particularly proximally and mesially (Tab. 1); and increased metathecal width (Fig. 12C). Further changes from the early form to the late form of

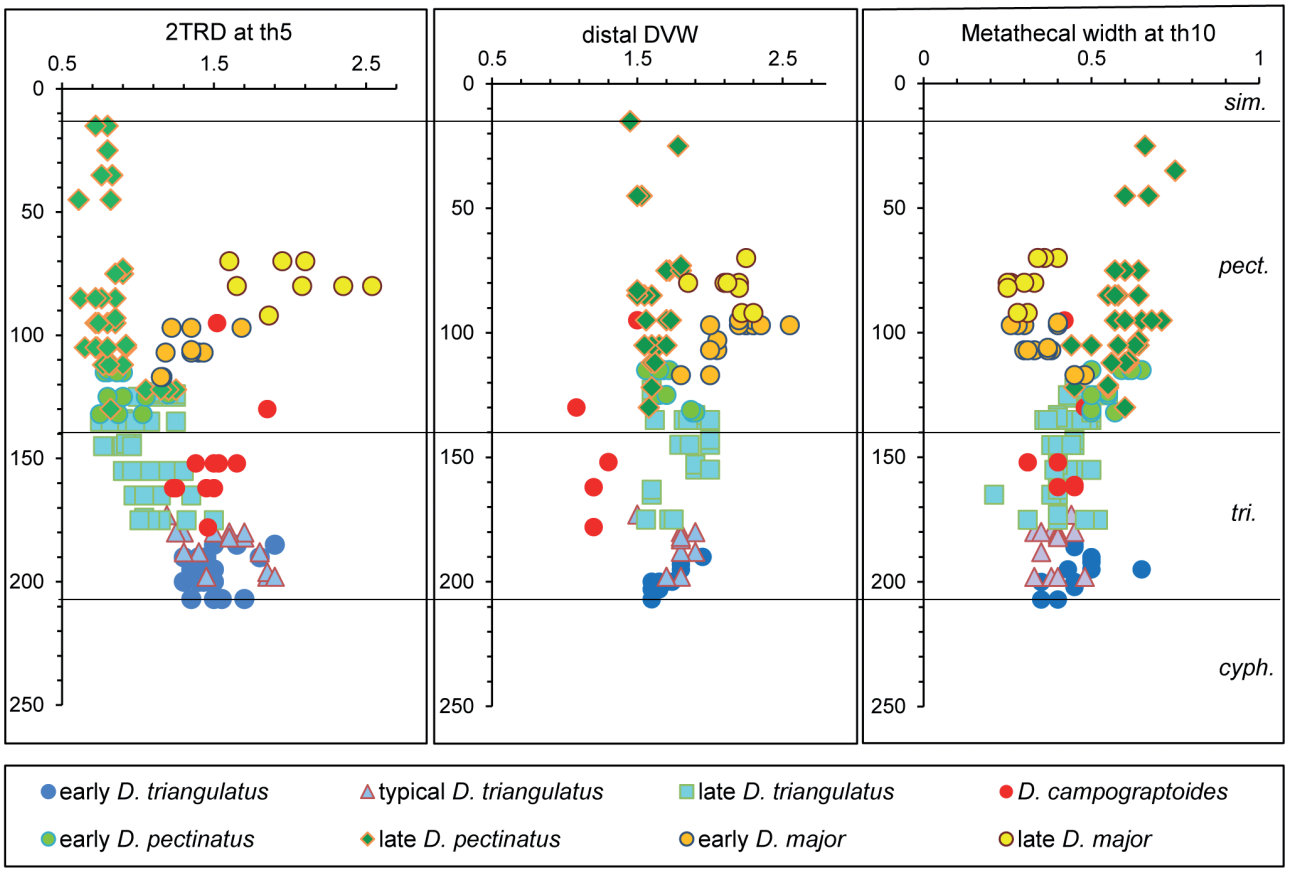

Figure 12. Some morphological trends observed in demirastritids of the *triangulatus* group in the Hlásná Třebaň section shown by plots of selected morphometric data *versus* stratigraphical level (vertical axis). • A – comparison of species and morphotypes using proximal thecal spacing (2TRD at th 5) of the specimen plotted against its stratigraphical level. • B – distal dorso-ventral width (DVW distal) versus stratigraphical level. • C – comparison of species and morphotypes through metathecal width of th10 versus stratigraphical level. Vertical scale refers to samples HT (205–207)–HT (0–20) listed on the left side of the section log in Fig. 2. Abbreviations: *cyph.* – *cyphus* Biozone; *tri.* – *triangulatus* Biozone; *pect.* – *pectinatus* Biozone; *sim.* – *simulans* Biozone.

D. pectinatus include further decrease in the curvature of the proximal part, lessening of the mesial to distal rhabdosome width (Fig. 12B and also Fig. 6F *versus* 6I) due to lower thecal inclination; further reduction in the number of sub-rastritiform proximal thecae; and further widening of the metathecae, particularly in the stratigraphically highest collections (Figs 8C, 12C). The widening of the metathecae in the late form of *D. pectinatus* is unlikely to be caused solely by more intense flattening of the rhabdosome because associated specimens *Demirastrites major* in the *pectinatus* Biozone possess rather slender thecae throughout.

As with *D. pectinatus*, there are two distinct forms of *Demirastrites major*, an early form and a late form. The early form (Figs 6E; 7D, E, H–L) occurs in the HT110–120, HT100–110 and HT90–100 samples, first appearing in the sample immediately above the highest occurrence of *D. triangulatus* (Fig. 2). The stratigraphically lowest specimens of *D. major* closely resemble the late form of *D. triangulatus*, including the possession of relatively a tightly coiled proximal part of the rhabdosome, but differ primarily in that specimens of early *D. major* commonly possess a larger number of parallel-sided proximal to mesial thecae, metathecae that are commonly slightly ventrally curved throughout, more pronounced lateral apertural processes, and more closely spaced distal thecae. There are clear morphological trends within the short range of the early form of *D. major* that further distinguish it from *D. triangulatus*, which also appear to change gradationally from the early to the late form of *D. major* (Figs 6B, C, J; 7A–C, F), which occurs in the HT90–100, 80–90 and 70–80 samples: increasing proximal 2TRD (Fig. 12A); increasing distal DVW (Fig. 12B); decreasing metathecal width mesially and distally (Fig. 12C); an increasing number of parallel-sided (but ventrally curved) proximal to mesial metathecae (Fig. 7); and a more gradual increase in DVW throughout the length of the rhabdosome (Tab. 1).

Demirastrites campograptoides, with its robust, relatively low and inclined distal thecae with rounded apertural hooks and short lateral processes, seems to be quite morphologically distinct from the other species of *Demirastrites* in this study. The limited data suggest that it may show an increase in its proximal 2TRD throughout at least part of its range but more data are required to support this apparent trend.

Although the morphological patterns described above have been documented only in a single stratigraphical succession, these observations lead us to propose that some of the apparent trends may represent anagenetic or cladogenetic events within the lineages. For example, the very strong similarities in many characters between the highest specimens of the late form of *D. triangulatus* and the early form of *D. pectinatus* suggest that the divergence of these lineages represents a speciation event that took place at the level recognized as the base of the *pectinatus* Biozone (Fig. 2, event 2). Whereas some characters change gradually through this event (*e.g.* mesial-distal metathecal width and reduction in number of proximal sub-rastritiform thecae), others (*e.g.* reduction in degree of proximal coiling) change abruptly. The same can be said of the apparent transition from late *D. triangulatus* to early *D. major* (Fig. 2, event 3), which involves some gradual (*e.g.* increasing proximal 2TRD, distal DVW, and increasing number of parallel-sided thecae) and some more abrupt (*e.g.* ventrally curved metatheca with more pronounced lateral apertural processes) changes marking the speciation event. In addition, several of the forms show more gradual changes within their individual ranges, which could be interpreted as anagenetic changes. Examples include: changes within the range of *D. triangulatus* (Fig. 2, event 4), including gradually decreasing proximal 2TRD, particularly within the range of the late form; gradually increasing proximal 2TRD within the range of *D. major* (Fig. 2, event 7); gradually increasing metathecal width, and further decreases in the number of sub-rastritiform proximal thecae within the range of *D. pectinatus* (Fig. 2, event 6). Limited material does not allow for any further insights into the evolutionary origin or anagenetic trends in *D. campograptoides* at this time.

It is important to reiterate that these trends have only been fully documented in a single section and must be tested in other sections that show a similarly complete record through this interval. The proposed anagenetic trends, in particular, could be the result of local ecophenotypic variation through the study section, rather than evolutionary trends within the species as a whole. In addition, the proposed phylogenetic relationships could be tested using cladistic analysis of species of *Demirastrites* together with other taxa that are likely to be closely related.

Conclusions

1) Lower Aeronian "triangulate monograptids" assigned to to the genus *Demirastrites* Eisel, 1912 are represented by *D. triangulatus* (Harkness), *D. major* (Elles & Wood), *D. pectinatus* (Richter) and *D. campograptoides* sp. nov. in the Prague Synform of the Barrandian area, Czech Republic. *Demirastrites extremus* (Sudbury, 1958) and *Demirastrites predecipiens* (Sudbury, 1958) have not been identified here and have been previously found only in Britain. Also ?*Demirastrites similis* (Elles & Wood, 1913) had been recorded solely from Britain until its recent discovery in Myanmar by Loydell & Aung (2017). *Demirastrites triangulatus separatus* (Sudbury 1958) is not considered here to be a distinct subspecies, and *Demirastrites raitzhainiensis* (Eisel, 1912) is regarded here to be a junior synonym of *D. triangulatus*. Specimens that are potentially assignable to *Demirastrites triangulatus separatus* and *D.*

triangulatus triangulatus exhibit morphological features and dimensions that fall within what we have observed to be a continuous range of variation of a single taxon, accounting for differences in mode of preservation of the type material and our collections. Differences between *Demirastrites raitzhainiensis* and *D. triangulatus* can be accounted for by the fact that the former has been strongly deformed by tectonic strain. In addition, *Demirastrites triangulatus fimbriatus* (Nicholson, 1868), which corresponds with *D. pectinatus* in all relevant morphological characters, dimensions and stratigraphical occurrence, is considered a junior synonym of the latter taxon.

2) Although our morphological data are derived mainly from only one section, they suggest the possibility that *D. triangulatus* underwent significant anagenetic changes throughout its range. This lineage then split at about the level of sample HT130–140 and gave rise to *D. pectinatus*, which marks the base of the *pectinatus* Biozone, which then underwent further anagenetic changes between its early and late forms. At a slightly later stage the *D. triangulatus* lineage underwent significant changes, giving rise, at the level of sample HT90–100, to *D. major*, which then saw further significant anagenetic changes before it became extinct in the middle *pectinatus* Biozone (Fig. 2). It is, however, possible that some of the changes interpreted here to be anagenetic evolutionary trends could be local ecophenotypic changes within the broader ranges of the taxa. Further comparative morphometric work and phylogenetic analysis using material from other regions will be required to test these hypotheses. *Demirastrites campograptoides* is a new species, to date recognized solely in collections from Hlásná Třebaň and Všeradice.

Acknowledgements

Petr Štorch greatly appreciates the financial support provided by the Czech Science Foundation through project 14-16124S, in-house support received from the Institute of Geology of the Academy of Sciences of the Czech Republic (RVO 67985831), and support provided by St. Francis Xavier University, Antigonish, Nova Scotia, through the James Chair Visiting Professorship during the 2018-2019 academic year. Michael J. Melchin acknowledges the financial support of a Natural Sciences and Engineering Research Council (Canada) Discovery Grant, as well as logistical support for fieldwork in the Arctic from the Polar Continental Shelf Project. We thank J. Fan and Q. Chen for supporting and facilitating our work in China, including access to Chinese graptolite collections and our joint study of Chinese sections, and also A. Lenz for providing some of his Yukon collections to MJM. We are indebted to V. Turek and L. Váchová who photographed the shale slab in Fig. 11 and Š. Manda and J. Kotek who assisted in the field. Finally, we thank D. K. Loydell and V. Sachanski for their helpful reviews of the manuscript.

References

Anhui Geological Survey 1982. *Graptolites of Anhui Province*. 166 pp. Anhui Science and Technology Publishing House, Hefei. [in Chinese]

Bjerreskov, M. 1975. Llandoverian and Wenlockian graptolites from Bornholm. *Fossils and Strata 8*, 1–94.

Bouček, B. 1953. Biostratigraphy, development and correlation of the Želkovice and Motol Beds of the Silurian of Bohemia. *Sborník Ústředního Ústavu geologického, Oddíl paleontologický 20*, 421–484.

Bulman, O.M.B. 1957. Proposed use of the plenary powers to designate for three taxa belonging to the Class Graptolithina lectotypes which will secure the continued use of the names concerned in their accustomed sense. *Bulletin of Zoological Nomenclature 13*, 313–317. DOI 10.5962/bhl.part.3567

Challinor, J. 1945. A graptolite lineage from North Cardiganshire. *Geological Magazine 82*, 97–106. DOI 10.1017/S0016756800078055

Chen, X. 1984. Silurian graptolites from southern Shaanxi and northern Sichuan with special reference to classification of Monograptidae. *Palaeontologia Sinica, New Series B 20*, 1–102. [in Chinese, with English summary]

Chen, X. & Lin, Y.-K. 1978. Lower Silurian graptolites from Tongzi, northern Guizhou. *Memoir of the Nanjing Institute of Geology and Palaeontology, Academia Sinica 12*, 1–106. [in Chinese, with English abstract]

Cooper, R.A. & Lindholm, K. 1990. A precise worldwide correlation of early Ordovician graptolite sequences. *Geological Magazine 127*, 497–525. DOI 10.1017/S0016756800015429

Cooper, R.A., Sadler, P.M., Munnecke, A. & Crampton, J.S. 2014. Graptoloid evolutionary rates track Ordovician-Silurian global climate change. *Geological Magazine 151*, 349–364. DOI 10.1017/S0016756813000198

Cullum, A.A. & Loydell, D.K. 2011. The Rhuddanian/Aeronian transition in the Rheidol Gorge, mid Wales. *Proceedings of the Yorkshire Geological Society 58(4)*, 261–266. DOI 10.1144/pygs.58.4.299

Dawson, D.H. 2007. *Phylogenetic study of the earliest Silurian Monograptus (Graptolithina) and related taxa, Cape Phillips Formation, Nunavut, Canada*. 176 pp. Master thesis. St. Francis Xavier University, Antigonish.

Eisel, R. 1899. Über die Zonenfolge Ostthüringischer und Vogtländischer Graptolithenschiefer. *Jahresberichte der Gesellschaft von Freunde der Naturwissenschaften in Gera 39/42*, 49–62.

Eisel, R. 1908. Über Verdrückungen thüringisch-sächsischer Graptolithenformen. *Zeitschrift für Naturwissenschaften. Organ des naturwissenschaftlichen Vereins für Sachsen und Thüringen, Halle AS 80*, 218–221.

Eisel, R. 1912. Über zonenweise Entwicklung der Rastriten und Demirastriten. *Jahresberichte der Gesellschaft von Freunde der Naturwissenschaften in Gera 53/54*, 27–43.

Elles, G.L. & Wood, E.M.R. 1913. A monograph of British graptolites. Part 9. *Monograph of the Palaeontographical Society 66(323)*, 415–486. DOI 10.1080/02693445.1913.12035561

Fan, J.-X., Chen, Q., Melchin, M.J., Sheets, H.D., Chen, Z.-Y., Zhang, L.-N. & Hou, X.-D. 2013. Quantitative stratigraphy of the Wufeng and Lungmachi black shales and graptolite evolution during and after the Late Ordovician mass extinction. *Palaeogeography, Palaeoclimatology, Palaeoecology 389*, 96–114. DOI 10.1016/j.palaeo.2013.08.005

Harkness, R. 1851. Description of the graptolites found in the black shales of Dumfriesshire. *Quarterly Journal of the Geological Society of London 7*, 58–65. DOI 10.1144/GSL.JGS.1851.007.01-02.16

Howe, M.P.A. 1983. Measurement of thecal spacing in graptolites. *Geological Magazine 120*, 635–638. DOI 10.1017/S0016756800027795

Hutt, J. E. 1975. The Llandovery graptolites of the English Lake District. Part 2. *Monograph of the Palaeontographical Society 129(542)*, 57–137.

Jaeger, H. & Schönlaub, H.P. 1977. Das Ordoviz/Silur-Profil im Nölblinggraben (Karnische Alpen, Österreich). *Verhandlungen der Geologischen Bundesanstalt 1977*, 349–359.

Jones, H., Zalasiewicz, J. & Rickards, R.B. 2002. Clingfilm preservation of spiraliform graptolites: Evidence of organically sealed Silurian seafloors. *Geology 30*, 343–346. DOI 10.1130/0091-7613(2002)030<0343:CPOSGE>2.0.CO;2

Jones, O.T. 1909. The Hartfell-Valentian succession in the district around Plynlimon and Pont Erwyd (North Cardiganshire). *Quarterly Journal of the Geological Society of London 65*, 463–537. DOI 10.1144/GSL.JGS.1909.065.01-04.32

Lapworth, C. 1873. On an improved classification of the Rhabdophora. *Geological Magazine 10(1)*, 500–504, 555–560. DOI 10.1017/S0016756800469256

Lenz, A.C. 1982. Llandoverian graptolites of the Northern Canadian Cordillera: *Petalograptus*, *Cephalograptus*, *Rhaphidograptus*, *Dimorphograptus*, Retiolitidae, and Monograptidae. *Life Sciences Contributions Royal Ontario Museum 130*, 1–154. DOI 10.5962/bhl.title.60100

Li, J.-J. 1995. Lower Silurian graptolites from the Yangtze Gorge district. *Palaeontologia Cathayana 6*, 215–344.

Loydell, D.K. 1993. Upper Aeronian and lower Telychian (Llandovery) graptolites from western mid-Wales. Part 2. *Palaeontographical Society Monograph 147(592)*, 56–180.

Loydell, D.K. 2012. Graptolite biozone correlation charts. *Geological Magazine 149*, 124–132. DOI 10.1017/S0016756811000513

Loydell, D.K. & Aung, K.P. 2017. The "Panghkawkwo graptolite bed" (Llandovery, Silurian), Myanmar and the location of the Sibumasu (or Sibuma) Terrane in the Silurian. *Palaeogeography, Palaeoclimatology, Palaeoecology 469*, 1–17. DOI 10.1016/j.palaeo.2016.12.028

Loydell, D.K., Frýda, J. & Gutiérrez-Marco, J.C. 2015. The Aeronian/Telychian (Llandovery, Silurian) boundary, with particular reference to sections around the El Pintado reservoir, Seville province, Spain. *Bulletin of Geosciences 90*, 743–794. DOI 10.3140/bull.geosci.1564

Loydell, D.K., Männik, P. & Nestor, V. 2003. Integrated biostratigraphy of the lower Silurian of the Aizpute-41 core, Latvia. *Geological Magazine 140*, 205–229. DOI 10.1017/S0016756802007264

Loydell, D.K., Walasek, N., Schovsbo, N.H. & Nielsen, A.T. 2017. Graptolite biostratigraphy of the lower Silurian of the Sommerodde-1 core, Bornholm, Denmark. *Bulletin of the Geological Society of Denmark (DGF) 65*, 135–160.

Melchin, M.J. 1989. Llandovery graptolite biostratigraphy and paleobiogeography, Cape Phillips Formation, Canadian Arctic Islands. *Canadian Journal of Earth Sciences 26*, 1726–1746. DOI 10.1139/e89-147

Melchin, M.J. & Holmden, C. 2006. Carbon isotope chemostratigraphy of the Llandovery in Arctic Canada: Implications for global correlation and sea-level change. *GFF 128(2)*, 173–180. DOI 10.1080/11035890601282173

Melchin, M.J., Lenz, A.C. & Kozłowska, A. 2017. Retiolitine graptolites from the Aeronian and lower Telychian (Llandovery, Silurian) of Arctic Canada. *Journal of Paleontology 91*, 116–145. DOI 10.1017/jpa.2016.107

Melchin, M.J., Sadler, P.M. & Cramer, B.D. 2012. The Silurian Period, 525–558. *In* Gradstein, F.M., Ogg, J.G., Smith, A.G. & Ogg, G.M. (eds) *The Geologic Time Scale 2012*. Elsevier, Amsterdam.

Melchin, M.J., Boom, A., Davies, J.R., De Weirdt, J., McIntyre, A.J., Morgan, G., Phillips, S., Russell, C., Vandenbroucke, T.R.A., Williams, M. & Zalasiewicz, J.A. 2016b. *Integrated stratigraphic study of the Rhuddanian-Aeronian (Llandovery, Silurian) boundary succession at Rheidol Gorge, Wales*. Abstracts of IGCP 591 Meeting, Ghent.

Melchin, M.J., Davies, J.R., De Weirdt, J., Russell, C., Vandenbroucke, T.R.A. & Zalasiewicz, J.A. 2018. *Integrated stratigraphic study of the Rhuddanian-Aeronian (Llandovery, Silurian) boundary succession at Rheidol Gorge, Wales: a preliminary report*. 16 pp. Open Report OR/18/39, British Geological Survey.

Melchin, M.J., Sheets, H.D., Mitchell, C.E. & Fan, J. 2016a. A new approach to quantifying stratigraphical resolution: application to global stratotypes. *Lethaia 50*, 407–423. DOI 10.1111/let.12193

Ni, Y.-N. 1978. Lower Silurian graptolites from Yichang, western Hubei. *Acta Palaeontologica Sinica 17*, 387–416. [in Chinese]

Nicholson, H.A. 1868. On the graptolites of the Coniston Flags; with notes on the British species of the genus *Graptolites*. *Quarterly Journal of the Geological Society of London 24*, 521–545. DOI 10.1144/GSL.JGS.1868.024.01-02.67

Obut, A.M., Sobolevskaya, R.F. & Bondarev, V.I. 1965. *Graptolity silura Taimyra*. 120 pp. Akademiya Nauk USSR, Sibirskoje Otdelenie, Institut Geologii i Geofiziki, Moskva. [in Russian]

Obut, A.M., Sobolevskaya, R.F. & Merkureva, A.P. 1968. *Graptolity Llandoveri v Kernakh Burovykh Skvazhin Norilskogo Rayona*, 162 pp. Akademiya Nauk USSR, Sibirskoje Otdelenie, Institut Geologii i Geofiziki, Moskva. [in Russian]

Obut, A.M., Sobolevskaya, R.F. & Nikolaev, A.A. 1967. *Graptolity i Stratigrafiya Nizhnego Silura Okrainnykh Podnyatii Kolymskogo Massiva,* 164 pp. Akademiya Nauk SSR, Sibirskoje Otdelenie, Institut Geologii i Geofiziki. Ministerstvo Geologii SSSR, Nauchno-Issledovatel'sky Institut Geologii Arktiki, Moskva. [in Russian]

Paškevičius, J. 1979. *Biostratigraphy and Graptolites of the Lithuanian Silurian*. 267 pp. Mokslas, Vilnius. [in Russian, with English summary]

Perner, J. 1897. *Études sur les Graptolites de Bohême. Part 3. section a.* 25 pp. Raimond Gerhard, Prague.

Piçarra, J.M., Robardet, M., Oliveira, J.T., Paris, F. & Lardeux, H. 2009. Graptolite faunas of the Llandovery "phtanites" at Les Fresnaies (Chalonnes-sur-Loire, southeastern Armorican Massif): Palaeontology and biostratigraphy. *Bulletin of Geosciences 84*, 41–50. DOI 10.3140/bull.geosci.1085

Přibyl, A. & Münch, A. 1942. Revize středoevropských zástupců rodu *Demirastrites* Eisel. *Rozpravy České akademie věd a umění, Třída 2 51(31)*, 1–29.

Richter, R. 1853. Thüringische Graptolithen. *Zeitschrift der Deutschen geologischen Gesellschaft 5*, 439–464.

Rickards, R.B. 1970. The Llandovery (Silurian) graptolites of the Howgill Fells, northern England. *Monograph of the Palaeontographical Society 123(524)*, 1–108.

Rickards, R.B., Hutt, J.E. & Berry, W.B.N. 1977. Evolution of the Silurian and Devonian graptoloids. *Bulletin of the British Museum (Natural History), Geology 28*, 1–120.

Sadler, P.M. 2004. Quantitative biostratigraphy: achieving finer resolution in global correlation. *Annual Review of Earth and Planetary Sciences 32*, 187–213. DOI 10.1146/annurev.earth.32.101802.120428

Sadler, P.M., Cooper, R.A. & Melchin, M.J. 2011. Sequencing the graptoloid clade: building a global diversity curve from local range charts, regional composites and global timelines. *Proceedings of the Yorkshire Geological Society 58(4)*, 329–343. DOI 10.1144/pygs.58.4.296

Sadler, P.M., Kemple, W.G. & Kooser, M.A. 2003. Contents of the compact disk – CONOP9 programs for solving the stratigraphic correlation and seriation problems as constrained optimization, 461–465. *In* Harries, P.J. (ed.) *High resolution approaches in stratigraphic paleontology*. Kluwer Academic Publishers, Dordrecht.

Schauer, M. 1971. Biostratigraphie und Taxionomie der Graptolithen des tieferen Silurs unter besonderer Berucksichtigung der tektonischen Deformation. *Freiberger Forschungshefte, C273 Paläontologie*, 1–185.

Shaw, A.B. 1964. *Time in stratigraphy*. 365 pp. McGraw Hill, New York.

Sheets, H.D., Mitchell, C.E., Izard, Z.T., Willis, J.M., Melchin, M.J. & Holmden, C. 2012. Horizon annealing a collection-based approach to automated sequencing of the fossil record. *Lethaia 45*, 532–547. DOI 10.1111/j.1502-3931.2012.00312.x

Štorch, P. 1994. Graptolite biostratigraphy of the Lower Silurian (Llandovery and Wenlock) of Bohemia. *Geological Journal 29*, 137–165. DOI 10.1002/gj.3350290204

Štorch, P. 2015. Graptolites from Rhuddanian-Aeronian boundary interval (Silurian) in the Prague Synform, Czech Republic. *Bulletin of Geosciences 90(4)*, 841–891. DOI 10.3140/bull.geosci.1568

Štorch, P. & Kraft, P. 2009. Graptolite assemblages and stratigraphy of the lower Silurian Mrákotín Formation, Hlinsko Zone, NE interior of the Bohemian Massif (Czech Republic). *Bulletin of Geosciences 84(1)*, 51–74. DOI 10.3140/bull.geosci.1077

Štorch, P., Manda, Š., Tasáryová, Z., Frýda, J., Chadimová, L. & Melchin, M.J. 2018. A proposed new global stratotype for Aeronian Stage of the Silurian System: Hlásná Třebaň section, Czech Republic. *Lethaia 51*, 357–388. DOI 10.1111/let.12250

Sudbury, M. 1958. Triangulate monograptids from the *Monograptus gregarius* Zone (Lower Llandovery) of the Rheidol Gorge (northern Cardiganshire). *Philosophical Transactions of the Royal Society of London, Series B 241*, 485–555. DOI 10.1098/rstb.1958.0011

Sudbury, M. 1959. *Monograptus triangulatus*. *Geological Magazine 96*, 171–172. DOI 10.1017/S0016756800060088

Sudbury, M. & Hutt, J. 2000. *Monograptus triangulatus separatus* Sudbury, 1958. *Atlas of Graptolite Type Specimens*, Folio 1.64.

Törnquist, S.L. 1899. Researches into the Monograptidae of the Scanian Rastrites Beds. *Lunds Universitets Årsskrifter 35*, 1–25.

Törnquist, S.L. 1907. Observations on the genus *Rastrites* and some allied species of *Monograptus*. *Lunds Universitets Årsskrifter (NS), Afd. 2, 3, 5*, 1–22.

Wilkinson, J. 2018. *Monograptus triangulatus fimbriatus* (Nicholson, 1868). *Atlas of Graptolite Type Specimens*, Folio 3.32.

Willefert, S. 1963. Les Graptolites du Silurien inferieur du jbel Eguer-Iguiguena (SW d'Ito anticlinorium de Kasba-Tadla-Azrou, Maroc central). *Notes et Mémoires du Service geologique, Rabat 177*, 1–70.

Zalasiewicz, J. 2007. *Monograptus triangulatus triangulatus* (Harkness, 1851). *Atlas of Graptolite Type Specimens*, Folio 2.92.

Zalasiewicz, J.A., Taylor, L., Rushton, W.A., Loydell, D.K., Rickards, R.B. & Williams, M. 2009. Graptolites in British stratigraphy. *Geological Magazine 146*, 785–850. DOI 10.1017/S0016756809990434